

Imaging in patients with cardiovascular implantable electronic devices: part 1—imaging before and during device implantation. A clinical consensus statement of the European Association of Cardiovascular Imaging (EACVI) and the European Heart Rhythm Association (EHRA) of the ESC

Ivan Stankovic ^{1*}, Jens-Uwe Voigt ², Haran Burri ³, Denisa Muraru^{4,5}, Leyla Elif Sade^{6,7}, Kristina Hermann Haugaa^{8,9}, Joost Lumens ¹⁰, Mauro Biffi¹¹, Jean-Nicolas Dacher ¹², Nina Ajmone Marsan¹³, Elise Bakelants ³, Charlotte Manisty ^{14,15}, Marc R. Dweck¹⁶, Otto A. Smiseth¹⁷, and Erwan Donal¹⁸

Reviewers: This document was reviewed by members of the 2020–2022 EACVI Scientific Documents Committee: Daniele Andreini, Magnus Bäck, Philippe B. Bertrand, Niall Keenan, and Danilo Neglia; and by the 2020–2022 EACVI President: Bernard Cosyns.

¹Clinical Hospital Centre Zemun, Department of Cardiology, Faculty of Medicine, University of Belgrade, Vukova 9, 11080 Belgrade, Serbia; ²Department of Cardiovascular Diseases, University Hospitals Leuven/Department of Cardiovascular Sciences, Catholic University of Leuven, Herestraat 49, Leuven 3000, Belgium; ³Cardiac Pacing Unit, Cardiology Department, University Hospital of Geneva, Geneva, Switzerland; ⁴Department of Medicine and Surgery, University of Milano-Bicocca, Milan, Italy; ⁵Department of Cardiology, Istituto Auxologico Italiano, IRCCS, Milan, Italy; ⁶University of Pittsburgh Medical Center, Heart and Vascular Institute, Pittsburgh, PA, USA; ⁷Department of Cardiology, University of Baskent, Ankara, Turkey; ⁸ProCardio Center for Innovation, Department of Cardiology, Oslo University Hospital, Rikshospitalet, Oslo, Norway; ⁹Faculty of Medicine Karolinska Institutet AND Cardiovascular Division, Karolinska University Hospital, Stockholm Sweden; ¹⁰Cardiovascular Research Center Maastricht (CARIM), Maastricht University, Maastricht, The Netherlands; ¹¹Department of Cardiology, IRCCS, Azienda Ospedaliero Universitaria Di Bologna, Policlinico Di S.Orsola, Bologna, Italy; ¹²Department of Radiology, Normandie University, UNIROUEN, INSERM U1096 - Rouen University Hospital, F 76000 Rouen, France; ¹³Department of Cardiology, Heart and Lung Center, Leiden University Medical Center, Leiden, The Netherlands; ¹⁴Department of Cardiovascular Imaging, Barts Heart Centre, Barts Health NHS Trust, London, UK; ¹⁵Institute of Cardiovascular Science, University College London, London, UK; ¹⁶Centre for Cardiovascular Science, University of Edinburgh, Little France Crescent, Edinburgh EH16 4SB, United Kingdom; ¹⁷Institute for Surgical Research, Oslo University Hospital and University of Oslo, Oslo, Norway; and ¹⁸University of Rennes, CHU Rennes, Inserm, LTSI-UMR 1099, Rennes, France

Received 14 October 2023; revised 15 October 2023; accepted 15 October 2023; online publish-ahead-of-print 20 October 2023

More than 500 000 cardiovascular implantable electronic devices (CIEDs) are implanted in the European Society of Cardiology countries each year. The role of cardiovascular imaging in patients being considered for CIED is distinctly different from imaging in CIED recipients. In the former group, imaging can help identify specific or potentially reversible causes of heart block, the underlying tissue characteristics associated with malignant arrhythmias, and the mechanical consequences of conduction delays and can also aid challenging lead placements. On the other hand, cardiovascular imaging is required in CIED recipients for standard indications and to assess the response to device implantation, to diagnose immediate and delayed complications after implantation, and to guide device optimization. The present clinical consensus statement (Part 1) from the European Association of Cardiovascular Imaging, in collaboration with the European Heart Rhythm Association, provides comprehensive, up-to-date, and evidence-based guidance to cardiologists, cardiac imagers, and pacing specialists regarding the use of imaging in patients undergoing implantation of conventional pacemakers, cardioverter defibrillators, and resynchronization

* Corresponding author. E-mail: future.ivan@gmail.com

therapy devices. The document summarizes the existing evidence regarding the use of imaging in patient selection and during the implantation procedure and also underlines gaps in evidence in the field. The role of imaging after CIED implantation is discussed in the second document (Part 2).

Keywords

multi-modality imaging • cardiovascular implantable electronic devices • pacemaker • cardiac resynchronization therapy • defibrillator

Introduction

More than 500 000 pacemakers and cardiac devices are implanted in the European Society of Cardiology (ESC) countries each year.¹ There is strong evidence that the implantation of cardiac devices improves patients' outcomes, whilst the evidence that cardiac imaging can improve patient selection and performance of these devices is growing.

The role of cardiac imaging in patients being considered for cardiovascular implantable electronic devices (CIEDs) is distinctly different from imaging in CIED recipients. In the former group, imaging can help identify specific or potentially reversible causes of heart block, the underlying tissue characteristics associated with malignant arrhythmias, and the mechanical consequences of conduction delays and can also aid challenging lead placements. Furthermore, this is an area of ongoing vibrant research aimed at identifying and filling evidence gaps to improve or refine strategies for selecting patients for implantation of different types of CIEDs.

On the other hand, cardiac imaging is required for standard indications in CIED recipients and to assess the response to device implantation, to diagnose immediate and delayed complications after implantation, and to guide device optimization.

This document is the first (Part 1) of two clinical consensus statements on imaging in patients with CIEDs and aims to provide comprehensive, up-to-date, and evidence-based guidance to cardiologists, cardiac imagers, and pacing specialists regarding the use of imaging in patients undergoing implantation of CIEDs: conventional anti-bradycardia pacemakers, implantable cardioverter defibrillators (ICDs), and cardiac resynchronization therapy (CRT) devices. The document summarizes the existing evidence regarding the use of imaging in patient selection and during the implantation procedure and also underlines gaps in evidence in the field. The role of imaging after device implantation is discussed in the second document (Part 2).

Methodology

This clinical statement is based on a review of the literature performed by the members of the writing group. The clinical advice is based upon the evidence and/or consensus of the writing group and is classified into several categories, as shown in *Table 1*.

General aspects of pre-implantation imaging






In the 2021 ESC guidelines on cardiac pacing and CRT and 2022 ESC guidelines for the management of patients with ventricular arrhythmias (VAs) and the prevention of sudden cardiac death (SCD), imaging is recognized as a crucial tool to assess cardiac function and also to detect the heterogenous conditions associated with conduction abnormalities, VA, and SCD.^{2,3} Accurately diagnosing the underlying disease state may have an impact on decisions regarding the type of CIED that will be implanted [e.g. conventional anti-bradycardia pacing or ICD in hypertrophic cardiomyopathy (HCM)] and lead to the initiation of disease-specific treatments [e.g. for transthyretin cardiac amyloidosis (CA) or Fabry disease] or both (e.g. ICD and immunosuppression in cardiac sarcoidosis) leading to improved patient outcomes. Regardless of the underlying disease state(s), the assessment of left ventricular (LV) systolic function by measuring LV

ejection fraction (LVEF) is a common step in the diagnostic workup of patients being considered for CIED implantation. An overview of the different LVEF cut-off values proposed by the current ESC guidelines to help guide which type of CIED should be implanted in various underlying conditions is shown in *Figure 1*. It should be noted that other imaging parameters, in particular assessments of myocardial scar, can also be used to refine decision-making in patients being considered for CIED implantation, particularly when LVEF is preserved (e.g. scar burden in HCM). In addition, pre-implantation cardiac imaging can also help identify the diverse, mainly anatomical reasons that might lead to challenging CIED lead placement (*Table 2*). In this introductory chapter, we discuss common aspects of pre-implantation cardiac imaging: the assessment of LV systolic function and the use of imaging in potentially challenging lead placement scenarios. Specific issues regarding the use of cardiac imaging to help guide the implantation of the different types of CIEDs will be discussed in the respective chapters of this document.

Assessment of LV systolic function

The assessment of LV size and function plays a pivotal role in patients undergoing device therapy. The general echocardiographic approach has been described in the European Association of Cardiovascular Imaging (EACVI)/American Society of Echocardiography (ASE) document on chamber quantification.⁴ In short, LV volumes and LVEF can be measured using 2D echocardiography (2DE) or 3D echocardiography (3DE). Calculations from linear measurements (e.g. Teichholz and Quinones methods) are no longer advised. The standard method for 2DE volume calculations is the biplane method of disk summation (modified Simpson's rule) where LV volumes are measured by tracing the endocardial borders in the apical four- and two-chamber views. Although the biplane method was mostly used to assess LVEF in the landmark ICD and CRT clinical trials, it is susceptible to inaccurate endocardial border tracing, and contrast agents use is advised to improve endocardial delineation when two or more contiguous LV segments are poorly visualized in apical views.⁴ Without contrast use, LVEF by 2DE and cardiovascular magnetic resonance (CMR, the current imaging

Table 1 Categories of clinical advice

	Definition	Symbol
Strength of advice	Clinical advice, based on robust published evidence	
	Clinical advice, based on uniform consensus of the writing group	
Area of uncertainty	May be appropriate, based on published evidence	
	May be appropriate, based on consensus within writing group	
	Area of uncertainty	

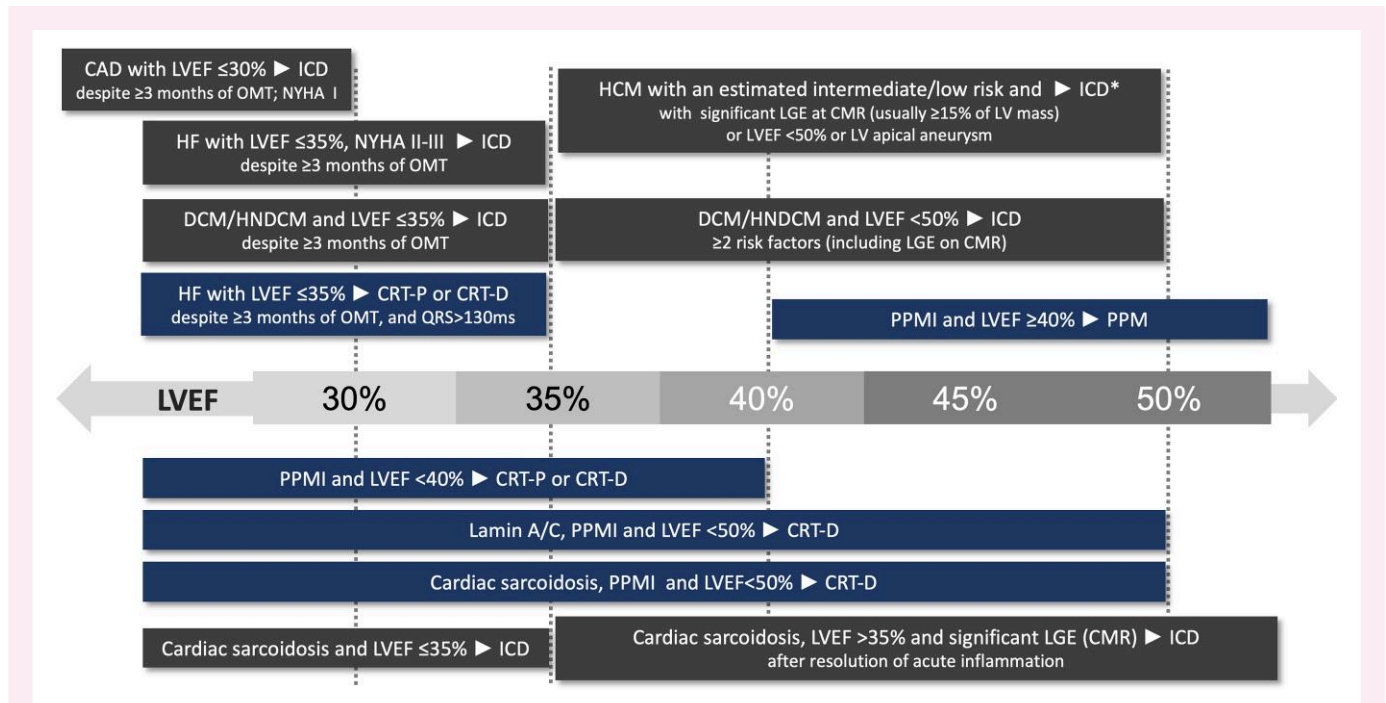


Figure 1 Guideline proposed LV ejection fraction cut-offs for cardiac implantable device implantation in various clinical scenarios (recommendations from the 2022 ESC guidelines for the management of patients with ventricular arrhythmias and the prevention of sudden cardiac death are shown in grey boxes, whilst those shown in blue boxes are from the 2021 ESC guidelines on cardiac pacing and cardiac resynchronization therapy). *Only imaging parameters are shown; dotted vertical lines represent LVEF cut-offs; CAD, coronary artery disease; CMR, cardiovascular magnetic resonance; CRT-P, cardiac resynchronization therapy with pacemaker; CRT-D, cardiac resynchronization therapy with defibrillator; DCM/HNDCM, dilated cardiomyopathy/hypokinetic non-dilated cardiomyopathy; ICD, implantable cardioverter defibrillator; HCM, hypertrophic cardiomyopathy; HF, heart failure; LGE, late gadolinium enhancement; LV, left ventricular, LVEF, left ventricular ejection fraction; NYHA, New York Heart Association class; OMT, optimal medical therapy; PPM, permanent pacemaker; PPMI, permanent pacemaker indication.

reference standard) may differ by $\geq 10\%$ EF units in up to 26% of patients.⁵ Furthermore, (semi)automated measurements based on speckle-tracking technology may be useful, as they reduce inter- and intra-observer variability. In general, caution is advised to avoid foreshortening of the LV in 2DE apical views, which typically results in volume underestimation and LVEF over- or underestimation.⁶ However, even when images are acquired by experienced operators taking care to maximize the LV long axis on apical views, foreshortening of the LV is frequently inevitable. LV volume quantification is further hampered by its reliance on the assumption that the LV cross section can be described by a stack of ellipsoidal disks, which can be inaccurate especially in the presence of local shape abnormalities such as aneurysms.⁷ These issues are of particular relevance, given that small differences in LVEF (5%) might determine whether a patient is a candidate for an ICD or not (Figure 1).

In patients with LV dysfunction undergoing ICD implantation, 3DE LVEF is an independent predictor of major arrhythmic events and improves arrhythmic risk prediction, with the potential to change decisions to implant an ICD in 20% of patients (most of them having 2DE LVEFs within $\pm 10\%$ from the threshold).⁸ Therefore, when the value of 2DE LVEF is close to the cut-off for ICD implantation ($\pm 5\%$)—particularly in patients with abnormal LV shape or extensive LV wall motion abnormalities—3DE or CMR may be helpful to confirm a patient's candidacy for primary prevention of ICD implantation (Figure 2).

Cardiac imaging in potentially challenging lead placement scenarios

Cardiac imaging reports should describe findings that may complicate CIED implantation (Table 2). Pre-procedural imaging may influence

the CIED insertion approach (transvenous right- or left-sided, epicardial) or help anticipate complications and define the most effective implantation technique.

CIED implantation in patients with complex adult congenital heart disease (ACHD) may be particularly technically demanding due to complex anatomy, both before and after repair procedures.⁹ These patients require a tailored approach, which should ideally be discussed by a heart team that includes imaging and ACHD specialists.

On the other hand, some mild-to-moderate complexity ACHDs, such as atrial septal defect (ASD), persistent left superior vena cava (PLSVC), or dextrocardia, may be unrecognized before the conduction disorder occurs^{10,11} (Figure 3). Whilst advanced screening for ACHD does not seem justified, some clinical signs (e.g. heart murmur, cyanosis, and digital clubbing) may raise suspicion of ACHD. In this situation, if a routine transthoracic echocardiography (TTE) examination is not sufficient to confirm or rule out clinically suspected ACHD, it is advisable to order appropriate imaging tests (e.g. CMR). PLSVC is usually an incidental finding, and it should be suspected in the presence of a dilated coronary sinus. The diagnosis is confirmed by computed tomography (CT), CMR, or an agitated saline echocardiography study through the patient's left antecubital vein if bubbles reach the coronary sinus before the right heart chambers (Figure 3). Use can be made of historical thoracic chest CT scans where these are available. In the presence of PLSVC, left-sided CIED implantation can be technically demanding. A right-sided approach is advised in these cases if a right superior vena cava is present without an innominate vein.¹² For these reasons, it seems prudent to use imaging to confirm or rule out PLSVC in patients with dilated coronary sinus before CIED implantation.

Patent foramen ovale (PFO) and ASD do not complicate CIED implantation *per se*. Still, care should be taken that the lead does not cross

into the left heart chambers, thereby increasing the risk of stroke or systemic embolization.¹³ In addition, PFO increases the risk of paradoxical septal embolism during transvenous lead extraction in patients with CIED-related infections.¹⁴ Whilst it does not seem necessary to use agitated saline study and provocative manoeuvres to systematically screen for PFO in patients undergoing CIED implantation, particular care should be taken in patients with known PFO or ASD, to ensure proper lead placement at implantation using multiple views.

Severe tricuspid regurgitation (TR) and right ventricular (RV) dilatation may interfere with lead placement and subsequent stability, whilst the presence of a mechanical tricuspid valve (TV) prosthesis may dictate the need for epicardial ventricular pacing or LV pacing through the coronary sinus.^{9–11} In a small randomized study in patients with severe TR, the ventricular lead was more easily and steadily located at the RV outflow tract (RVOT) septum than at the RV apex with shorter fluoroscopy time and lower incidence of intra-procedural dislodgement.¹⁵

Exceptionally, prominent embryonic remnants in the right atrium may pose a challenge to pacemaker lead placement.¹⁶ A prominent Eustachian valve, Chiari network, and Thebesian valve are occasionally seen in the right atrium as fenestrated membranes, ridges, or webs sometimes dividing the chamber into two cavities (Figure 3). On occasion, these structures may entrap a pacemaker lead within the right atrium or interfere with coronary sinus cannulation, resulting in prolonged procedure times, increased radiation exposure, failed lead implantation, or the surgical management of complication.^{17,18}

If TTE cannot provide sufficient information for pre-procedural planning, transoesophageal echocardiography (TOE), CT, or CMR imaging can be used to depict complex cardiac anatomy or vascular abnormalities.

Clinical advice

It is advised to routinely assess LV systolic function in patients undergoing CIED implantation.



The echocardiographic 2D biplane method of disk summation is the standard method to calculate LVEF.



In patients with good acoustic windows, extensive LV wall motion abnormalities or borderline LVEF (i.e. $\pm 5\%$ around the cut-off for ICD implantation), 3D echocardiography, if available, is the preferred method to measure LVEF by ultrasound.



If poor echocardiographic windows preclude a reliable assessment of LVEF, contrast echocardiography or CMR is advised.



Pre-implantation cardiac imaging reports should include the description of findings that may complicate CIED implantation.



Cross-sectional imaging with CT or CMR is advised in patients with suspected persistent left-sided SVC.



Imaging of patients undergoing CIED implantation: RV pacing vs. CRT

In the 2021 ESC guidelines on cardiac pacing and CRT, cardiac imaging is recommended in patients with symptomatic bradycardia to evaluate the presence of structural heart disease, to determine LV systolic function, and to diagnose potential causes of conduction disorders.²

Whilst degenerative conduction disease and coronary artery disease (CAD) are considered the most frequent causes of atrioventricular block (AVB) in elderly patients,² an underlying aetiology for AVB is not identified during standard clinical pre-implantation assessment in approximately half of the young–middle-aged patients.¹⁹ Of note, young pacemaker-treated patients with AVB have a three- to four-fold higher rate of the composite of death, hospitalization for heart failure (HF), VA, or aborted SCD when compared with a cohort of matched controls.²⁰ In line with this, by the 2021 ESC guidelines, myocardial tissue characterization with multi-modality imaging should be considered for the diagnostic workup of specific pathologies associated with conduction disorders requiring pacemaker implantation, especially in patients younger than 60 years.² This age cut-off is provisional, as some cardiac conditions associated with conduction disorders may be more frequent in elderly patients (e.g. transthyretin CA).

Assessment of structural heart disease and the potential aetiology of conduction abnormalities

Whilst echocardiography alone may be sufficient for the routine assessment of global and regional LV systolic function in most patients, multi-modality imaging may be needed to diagnose different congenital or acquired cardiac pathologies associated with conduction disorders. Figure 4 illustrates several important roles for cardiac imaging in the assessment of patients presenting with symptomatic bradycardia. Together with clinical data, a comprehensive multi-modality imaging assessment may identify potentially reversible causes of conduction abnormalities (e.g. acute ischaemia, inflammation, or infection) or previously undiagnosed cardiomyopathies or heart valve disease, which may vary widely in phenotype and clinical expression. Furthermore, imaging plays a role in determining the most appropriate type of CIED for a specific patient—those with conduction disorders will be treated with conventional anti-bradycardia pacing or CRT (with or without defibrillator capability) depending predominantly not only on LV systolic function but also on other imaging parameters, in particular the extent of myocardial scar. Finally, the presence of clinical or imaging red flags, regardless of LV systolic function, should trigger multi-modality imaging protocols to identify previously unrecognized cardiac or multi-systemic diseases in patients presenting with AVB thereby enabling disease-specific treatment (Table 3).

Identifying the AVB aetiology should ideally be performed prior to CIED implantation, especially if CMR is part of the diagnostic algorithm. However, this may not be always possible due to time constraints or limited availability of advanced imaging modalities or genetic testing; therefore, the diagnostic process can be completed after CIED implantation.

In the following, we briefly summarize the imaging approach to patients with various cardiac pathologies leading to conduction abnormalities. Of note, according to the 2023 ESC guidelines for the management of cardiomyopathies, contrast CMR is recommended in patients with cardiomyopathy at initial assessment.²¹ This means that the majority of these patients will have had prior imaging for review during consideration of device implantation. Further details can be found in the respective ESC and EACVI scientific documents.^{21–23}

Acute myocardial ischaemia

High-degree atrioventricular (AV) block most frequently occurs in patients with acute inferior or inferolateral myocardial infarctions, but it may also complicate anterior infarctions.²⁴

If AV block does not resolve after revascularization or spontaneously (within a waiting period of at least 5 days), permanent cardiac pacing is indicated.²

Table 2 Imaging findings associated with potentially challenging CIED implantation

	Preferred imaging modalities	Relevance for CIED implantation
Atrial and ventricular septal defects	TTE/TOE, CMR/CT (sinus venosus defects)	<ul style="list-style-type: none"> Misplacement of the lead in the left heart during implantation Risk of paradoxical embolization during lead extraction for CIED-related infection Difficult endocardial pacing at the site of repair (fibrosis or prosthetic material)
Persistent left superior vena cava*	TTE with agitated saline injection from the left antecubital vein, CT/CMR	<ul style="list-style-type: none"> Left-sided approach frequently challenging Right-sided approach preferred (if the presence of a right SVC is confirmed by venography or CT/CMR)
Central vein obstruction	Direct and CT venography	<ul style="list-style-type: none"> Planning appropriate (technically demanding and riskier) procedures when central veins are actually occluded
Dextrocardia	CXR, fluoroscopy	<ul style="list-style-type: none"> Difficult fluoroscopic orientation The possibility of associated cardiac defects
Severe tricuspid regurgitation	TTE, TOE, CMR	<ul style="list-style-type: none"> Difficult lead placement (TR jet, dilated RV)
Mechanical tricuspid valve prosthesis	TTE, TOE	<ul style="list-style-type: none"> LV pacing through the coronary sinus or epicardial ventricular pacing is required
Anatomic variants, congenital, or acquired anomalies of the coronary sinus	CT, CMR	<ul style="list-style-type: none"> Pre-procedural planning in cases with previously failed coronary sinus cannulation
Prominent embryonic remnants	TTE, TOE, CT, CMR	<ul style="list-style-type: none"> Possible entrapment of the pacemaker lead within the right atrium

*In the presence of a dilated coronary sinus, it is advisable to confirm or rule out the presence of persistent left superior vena cava.

CIED, cardiovascular implantable electronic device; CMR, cardiovascular magnetic resonance; CT, computed tomography; CXR, chest X-ray; RV, right ventricle; SVC, superior vena cava; TOE, transoesophageal echocardiography; TR, tricuspid regurgitation; TTE, transthoracic echocardiography.

Infective endocarditis

Conduction abnormalities are uncommon complications of infective endocarditis and should always raise suspicion of perivalvular extension of the infection and an aortic root abscess²⁵ (Figure 5). Due to the proximity of the AV node to the non-coronary aortic cusp and the anterior mitral leaflet, complete AV block is most often associated with aortic or mitral valve endocarditis.²⁵ The sensitivity of TTE for the detection of perivalvular complications of infective endocarditis is relatively low and the use of other imaging modalities, including TOE, CT, nuclear imaging positron emission tomography (PET)/CT, and single-photon emission CT (SPECT)/CT is advised, particularly in patients with clinically suspected prosthetic valve endocarditis²⁶ (Figure 6).

Severe aortic stenosis

Conduction abnormalities are common findings in patients with aortic valve disease, particularly in the presence of extensive valve calcifications and LV dysfunction.^{27,28}

Whilst permanent pacemaker implantation for conduction disturbances is relatively rare after isolated surgical aortic valve replacement (SAVR),²⁹ new-onset left bundle branch block (LBBB) and advanced AV block requiring permanent pacemaker implantation are common complications of transcatheter aortic valve implantation (TAVI).³⁰ The risk of pacemaker dependency after TAVI is influenced by several patient- and procedure-related factors, some of which can be assessed by CT.^{31,32} Anatomic factors predisposing to pacemaker dependency after TAVI include aortic valve calcification,³³ a larger annulus perimeter,³² a shorter membranous septum length,³⁴ LV outflow tract (LVOT) calcifications under the left coronary cusp, and a difference between membranous septum length and implantation depth of ≥ 3 mm.^{31,32} Membranous septum length is measured on

pre-procedural CT coronal views as the perpendicular distance from the annular plane to the beginning of the muscular septum, whilst implantation depth is measured at the final aortic angiogram as the distance between the lower end of the transcatheter heart valve frame and the lowest part of the non-coronary cusp.³¹ Lower implantation depth and oversizing have been identified as procedural factors associated with an increased risk of permanent pacemaker implantation following TAVI.³² There is currently no evidence to support pacemaker implantation prior to TAVI or extended rhythm monitoring after SAVR/TAVI based on pre-interventional imaging data.

Myocarditis

Patients with acute myocarditis uncommonly present with high-degree AV block. In a retrospective study of >30 000 patients with acute myocarditis, the incidence of high-degree AV block was 1.1% with only a minority of these (23.5%) requiring a permanent pacemaker.³⁵ However, Mobitz II or third-degree AV block can be seen in ~25% of patients with giant cell myocarditis.^{36,37} Early diagnosis in patients with unexplained high-degree AV block (particularly in those younger than 60 years) is worthwhile,² as they may benefit from immunosuppressive therapy.³⁸

The diagnosis of definite myocarditis has traditionally relied on endomyocardial biopsy. However, multi-parametric CMR imaging allows non-invasive tissue characterization and is now often used clinically to make a diagnosis of myocarditis without the need for biopsy. According to the 2018 Lake Louise criteria,³⁹ a CMR diagnosis of myocarditis is based on at least one T1-based criterion [increased myocardial T1 relaxation times, extracellular volume fraction, or late gadolinium enhancement (LGE)] with at least one T2-based criterion (increased myocardial T2 relaxation times, visible myocardial oedema, or increased T2 signal intensity ratio).

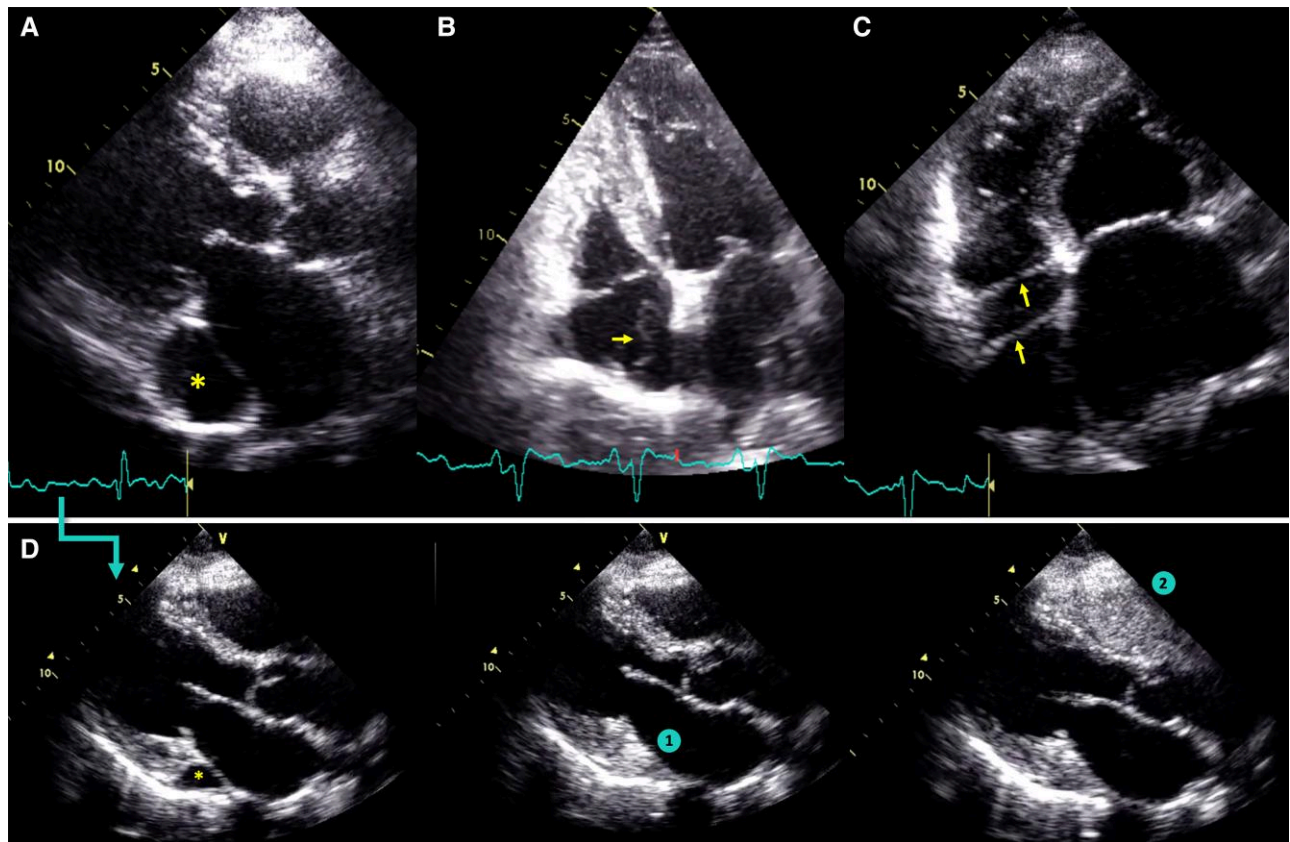


Figure 3 Echocardiographic findings indicating potentially challenging device implantation. (A) A dilated coronary sinus due to PLSVC, as demonstrated by an agitated saline study through the patient's left antecubital vein (D)—note that the bubbles are appearing in the coronary sinus (1) before showing in the right heart (2). (B) A prominent, mobile, net-like structure in the right atrium (Chiari network) in a patient with second-degree heart block. (C) Cor triatriatum dexter in a patient being considered for an implantable cardioverter-defibrillator.

pattern of diffuse subendocardial or transmural LGE (including hyper-enhancement of the atrial walls), abnormal gadolinium kinetics (difficulties in nulling the myocardium), and increased native T1 and extracellular volume.^{23,41} Whereas these typical echocardiographic or CMR findings are suggestive of CA, non-invasive diagnosis of ATTR-CA also requires bone scintigraphy and increased myocardial uptake of a bisphosphonate-based radiotracer (uptake equal to/greater than bone uptake) in the absence of a monoclonal gammopathy (light chain amyloidosis) (Figure 9).^{23,41}

Hypertrophic cardiomyopathy

Registry data indicate that up to 10% of patients with HCM require permanent pacemaker implantation because of conduction disorders.⁴² According to the 2021 ESC guidelines on cardiac pacing, AV sequential pacing with short AV delay may be considered in patients with HCM in sinus rhythm who have other pacing or ICD indications if drug-refractory symptoms or baseline or provokable LVOT gradients of ≥ 50 mmHg are present.² Further, according to the 2023 ESC guidelines on cardiomyopathies, sequential AV pacing, with optimal AV interval to reduce the LVOT gradient or to facilitate medical treatment with beta-blockers and/or verapamil, may be considered in selected patients with resting or provokable LVOT obstruction of ≥ 50 mmHg, sinus rhythm, and drug-refractory symptoms, who have contraindications for septal reduction therapies or are at high risk of developing heart block following septal reduction therapies.²¹

The mechanisms behind the beneficial effects of AV sequential pacing in HCM include asynchronous LV activation and premature septal

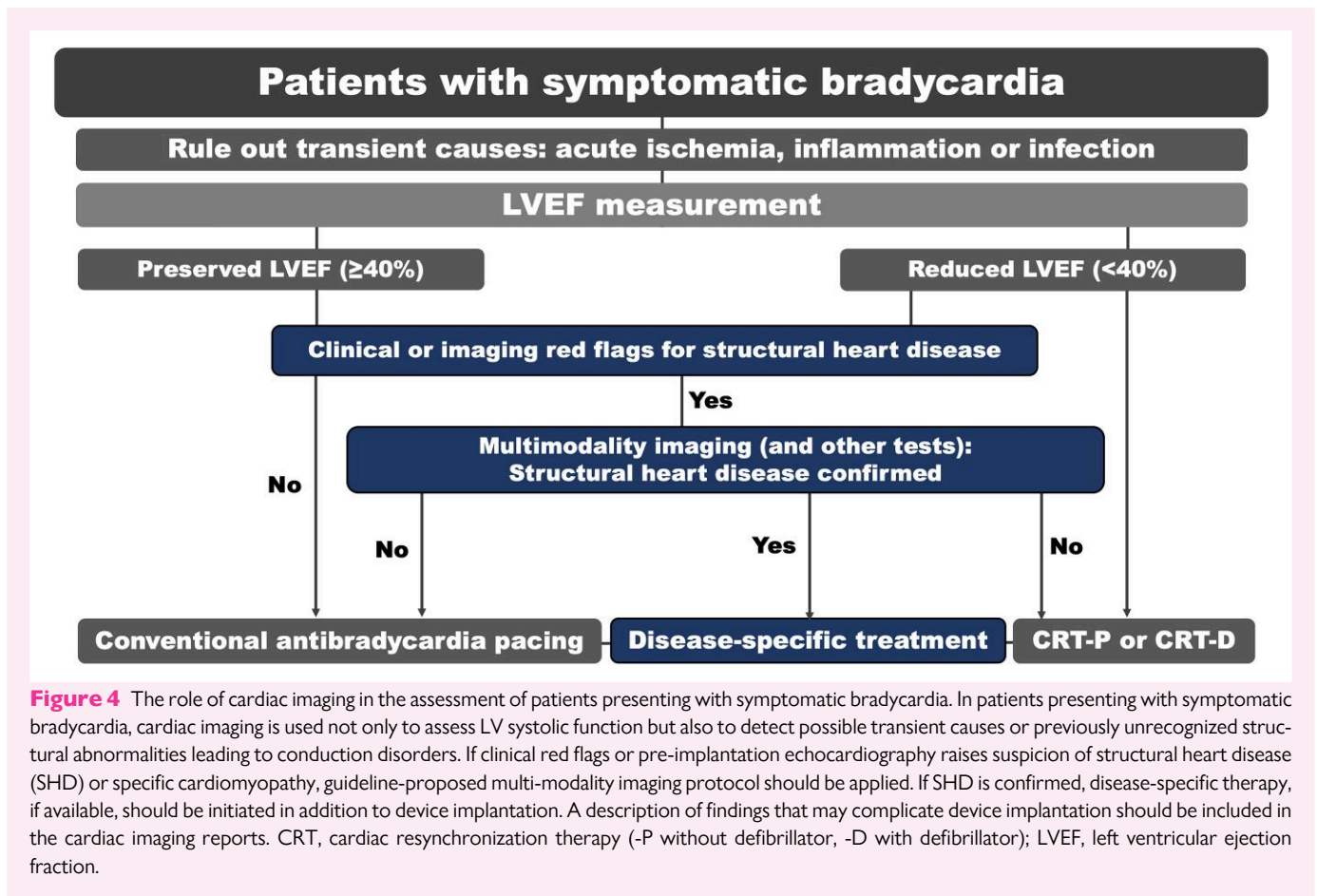
thickening, interactions with LV filling, negative inotropic effects with reduced hypercontractility of the LV, limitation of abnormal mitral valve motion, and LV remodelling.⁴³ Echocardiography can be used during AV delay optimization to assess changes in LVOT pressure gradient and LV filling patterns (Figure 10). Since the success of the procedure depends on full ventricular capture, AV delay must be short enough to fully capture the LV from the RV apex and also long enough to allow the atrial contribution to LV filling.⁴³ In clinical practice, AV delay optimization is carried out in a step-by-step fashion using surface electrocardiography (ECG) and TTE. The programmed AV delay should be changed gradually until reaching an optimal value defined as the longest AV delay that preserves both full ventricular capture (no fusion beats on ECG) and LV filling (no A-wave truncation on the pulsed-wave Doppler of the mitral inflow).

The use of imaging in risk stratification for SCD in HCM will be discussed in a subsequent section of this document. However, if a patient is being considered for pacing for LVOT obstruction, CMR for scar assessment is advised to guide device selection (conventional pacemaker or dual-chamber ICD).

Fabry disease

In an international survey comprising 714 patients with Fabry disease, conduction abnormalities were observed in 16% of patients, whilst 3% had a permanent pacemaker.⁴⁴

Echocardiographic features of the disease include biatrial enlargement, LV hypertrophy (concentric, asymmetrical septal, or apical),



increased papillary muscle thickness, LV diastolic dysfunction, and RV hypertrophy⁴⁵ (Figure 8). Abnormal segmental longitudinal strain in the basal and mid-inferolateral LV walls may precede thinning of these segments. On CMR, low native T1 values are characteristic, whilst basal non-infarct inferolateral LGE can be observed in approximately half of the patients with Fabry disease.⁴⁶

Dilated cardiomyopathy

If previously unknown and unexplained LV or biventricular dilatation and systolic dysfunction (EF < 40%) are discovered in a patient with an indication for permanent pacemaker implantation, the patient will be treated with a CRT device rather than with conventional anti-bradycardia pacing.² If the clinical scenario permits, then decision-making regarding the type of CIED required should involve heart team discussions after a thorough diagnostic workup and a minimum of 3 months of optimal medical therapy. In the pre-implantation workup, cardiac imaging is used to rule out ischaemic heart disease and also to detect the presence and extent of myocardial oedema, scarring, fibrosis, and infiltration in the dysfunctional myocardium.²⁰ According to the 2022 ESC guidelines, CMR with LGE should be considered in patients with dilated cardiomyopathy for assessing the aetiology and the risk of VA/SCD.³ If possible, CMR is advised prior to CIED implantation to avoid artefacts and also device-related safety issues (particularly if non-CMR conditional CIED will be implanted).

Haemochromatosis

Conduction disorders are seen in around 2% of haemochromatosis patients, whilst the most common cardiovascular manifestations of

haemochromatosis include arrhythmias, congestive HF, and pulmonary hypertension.^{23,47} CMR is the method of choice for assessing patients with suspected haemochromatosis, as T2-star (T2*) mapping can reliably identify and quantify myocardial iron accumulation.^{23,46}

Chagas disease

Chagas disease, caused by the protozoan *Trypanosoma cruzi*, is an important cause of bradyarrhythmias and pacemaker implantation in endemic areas.⁴⁸

The disease is characterized by atrial and VAs, conduction abnormalities, HF, thromboembolic events, and sudden death.⁴⁸ Cardiac imaging typically reveals thinning of the LV walls (most commonly seen in the basal inferolateral and lateral walls), apical ventricular aneurysms (with or without thrombi), impaired LV systolic function, and pericardial effusions.⁴⁸





Cardiac tumours

Cardiac tumours are exceedingly rare but may cause a wide spectrum of arrhythmias and conduction abnormalities, depending on the type of the tumour and the site of involvement.⁴⁹ For instance, cardiac fibromas have a propensity to cause VA, whilst cystic tumours of the AV node can cause sudden death despite pacemaker implantation. Although multi-modality imaging, particularly non-invasive tissue characterization with CMR imaging, can provide valuable information regarding the nature of the mass, histopathological characterization remains the diagnostic gold standard.⁵⁰ Besides CMR, a structured imaging approach to patients with a possible cardiac tumour may include TTE, TOE, contrast echocardiography, CT, and PET.⁵⁰

Imaging in temporary cardiac pacing

Temporary pacing wire insertion is usually performed under fluoroscopic guidance. Vascular ultrasound is very useful to guide central venous access, and echocardiography can be used to help temporary pacing lead positioning if fluoroscopy is not available.⁵¹ Ultrasound-guided jugular vein puncture involves identification of the internal jugular vein (confirmed by compressibility of the vessel), puncture of the vein, and confirmation of the correct position of the wire in the internal jugular vein lumen (Figure 11). Echocardiography-guided temporary pacing lead positioning is ideally performed from the subcostal window by continuous echo monitoring of the catheter pathway, from the right atrium through the TV to the RV apex (Figure 11).

Clinical advice

- If clinical data or pre-implantation TTEs raise suspicion of structural heart disease or specific cardiomyopathy, it is advised to evaluate the patient using the ESC guideline-proposed diagnostic algorithms. 
- If CMR is part of the diagnostic algorithm, it is advised to perform this examination prior to CIED implantation. 
- Echocardiography and ECG are useful during AV delay optimization to assess changes in LVOT pressure gradient and LV filling patterns in patients with hypertrophic obstructive cardiomyopathy and AV sequential pacing. 
- Vascular ultrasound is useful to guide central venous access and echocardiography can be used to help pacing lead positioning if fluoroscopy is not available. 

Imaging of patients undergoing implantation of cardioverter defibrillators

SCD may be the first manifestation of previously unrecognized CAD or cardiomyopathies, and multi-modality imaging has an essential role in the evaluation of structural heart disease of survivors. Most survivors will receive ICD therapy for secondary prevention unless a reversible cause of SCD is clearly identified.³ On the other hand, although the causes of SCD vary from frequent cardiomyopathies to rare channelopathies, decisions regarding primary prevention ICD therapy were almost solely based on reduced LVEF. The undeniable role of LVEF originates from the landmark ICD trials in which LVEF \leq 35%, usually assessed by 2D echocardiography, was the main inclusion criterion.⁵² However, it has a modest predictive accuracy, especially in patients with non-ischaemic cardiomyopathies,⁵³ and in the 2022 ESC guidelines, a balanced, more personalized approach combining clinical, imaging, and genetic data was proposed.³ Various cardiac imaging modalities allow visualization of tissue characteristics (often myocardial scar/fibrosis) that can be associated with VA in a broad spectrum of cardiomyopathies, but the lack of data from randomized trials currently limits their routine use for the prediction and prevention of VA and SCD. Using CMR scar as a risk indication tool in non-ischaemic cardiomyopathy with LVEF \leq 35% (on any imaging modality) is being tested in the ongoing

BRITISH randomized controlled trial (ClinicalTrials.gov Identifier: NCT05568069).

Imaging for identifying tissue characteristics that can be associated with VA

Assessment of myocardial scar and fibrosis, mechanical dispersion, inflammation, denervation, and impaired perfusion have all shown superiority to LVEF measurements in risk-stratifying patients for SCD in observational studies (Figure 12). LGE on CMR represents the non-invasive reference standard for the visualization and quantification of replacement myocardial fibrosis. The presence and extent of LGE are strongly associated with VA in both ischaemic and non-ischaemic cardiomyopathies.^{54,55} Furthermore, in patients with ischaemic cardiomyopathy, the size of the peri-infarct grey (border) zone, composed of a mixture of normal myocardium and fibrosis, is independently associated with VA, even after accounting for total myocardial scar burden.⁵⁶ Non-focal, diffuse myocardial fibrosis, often encountered in non-ischaemic cardiomyopathies, quantified by myocardial native T1 mapping and extracellular volume calculation, is also predictive of VA even in the setting of normal LVEF and in the absence of LGE.⁵⁷ The superiority of a CMR-guided management strategy for ICD insertion in patients with LVEF 36–50%, based on the presence of scar or fibrosis, to the current strategy based around an LVEF \leq 35% is being tested in the ongoing CMR GUIDE trial.⁵⁸

The presence of myocardial scar or fibrosis can be indirectly evaluated by assessing their functional consequences using myocardial strain and mechanical dispersion on speckle-tracking strain echocardiography or less often by CMR feature tracking analysis. GLS was independently associated with an increased risk of VA and the first appropriate ICD therapy in an unselected cohort of ICD patients with structural heart disease.⁵⁹ The ability of mechanical dispersion to predict VAs has been shown in patients with long QT syndrome,⁶⁰ post-myocardial infarction,^{61,62} and familial dilated cardiomyopathy.⁶³ There are currently no randomized controlled trials reported or in progress to provide evidence for the superiority of either GLS or mechanical dispersion over LVEF in VA or SCD prediction.

Nuclear imaging techniques have the ability to depict sympathetic denervation, perfusion defects, and cardiac inflammation and thus identify the risk for VA and SCD. Cardiac scintigraphy with the 123-iodine-labelled meta-iodobenzylguanidine (123I-MIBG), an analogue of noradrenaline, allows evaluation of cardiac sympathetic activity.⁶⁴ A heart-to-mediastinum ratio of <1.6 , calculated as 123I-MIBG accumulation in the heart divided by that in the mediastinum, has been identified as a risk factor for VA and SCD in both ischaemic and non-ischaemic cardiomyopathies.⁶⁵ Similarly, in ischaemic cardiomyopathy, sympathetic denervation assessed using 11-carbon-meta-hydroxyephedrine PET predicted SCD independently of LVEF and infarct volume.⁶⁶ Amongst patients with CAD and LVEF $>$ 35%, the extent of stress perfusion defects on SPECT myocardial perfusion imaging was associated with an increased risk of SCD.⁶⁷ Myocardial perfusion defects in patients with cardiac sarcoidosis can represent areas of scar or inflammation, whilst 18F-FDG PET identifies areas of pathologic glucose uptake and myocardial inflammation.³⁸ Patients with cardiac sarcoidosis with both focal perfusion defects and corresponding areas of inflammation (FDG uptake) were at higher risk of death or ventricular tachycardia (VT) than those with either perfusion defects or inflammation alone.⁶⁸

Recently, cardiac CT (CCT) has emerged as a promising method for identifying the substrate of malignant arrhythmias and in planning radio-frequency catheter ablation (RFCA) for refractory VT.^{69,70} In patients with contraindication to CMR, CCT identification of myocardial fibrosis was feasible and accurate vs. electro-anatomical mapping (EAM) during RFCA procedure.⁷¹ Finally, a pilot study suggested that CCT might be a

Table 3 Clinical red flags for suspecting some uncommon cardiac or multi-systemic diseases in patients presenting with unexplained conduction disorders

	Clinical red flags	Imaging modalities	Clinical relevance
Cardiac sarcoidosis	<ul style="list-style-type: none"> Unexplained AV block in younger patients (<60 years) Known extracardiac sarcoidosis 	TTE, CMR, PET	<ul style="list-style-type: none"> Specific treatment Lower threshold for ICD or CRT-D implantation
Cardiac amyloidosis	<ul style="list-style-type: none"> Carpal tunnel syndrome Spinal stenosis Peripheral neuropathy Low voltage (ECG) 	TTE, SPECT, CMR	<ul style="list-style-type: none"> Specific treatment
Hypertrophic cardiomyopathy	<ul style="list-style-type: none"> Positive family history High voltage (LVH) and/or repolarization abnormalities on ECG Systolic heart murmur 	TTE, CMR	<ul style="list-style-type: none"> Reduction of LVOT pressure gradient with AV sequential pacing Lower threshold for ICD Specific treatment
Fabry disease	<ul style="list-style-type: none"> Angiokeratoma Cornea verticillata Short PR interval Renal failure, proteinuria Juvenile/cryptogenic CVI Neuropathic pain 	TTE, CMR	<ul style="list-style-type: none"> Specific treatment
Haemochromatosis	<ul style="list-style-type: none"> Skin pigmentation Liver cirrhosis Skin bronzing Diabetes mellitus ↑ transferrin saturation 	TTE, CMR: T2-star mapping	<ul style="list-style-type: none"> Specific treatment
Chagas disease	<ul style="list-style-type: none"> Endemic countries GIT complications (megaesophagus, megacolon) Neurologic complications 	TTE, CMR	<ul style="list-style-type: none"> Specific treatment Lower threshold for ICD

AV, atrioventricular; CMR, cardiovascular magnetic resonance; CRT-D, cardiac resynchronization therapy with defibrillator; CT, computed tomography; CVI, cerebrovascular insult; ECG, electrocardiogram; GIT, gastrointestinal tract; ICD, implantable cardioverter defibrillator; LVH, left ventricular hypertrophy; LVOT, left ventricular outflow tract; PET, positron emission tomography; SPECT, single-photon emission computed tomography; TTE, transthoracic echocardiography.

useful tool for planning, guidance, and follow-up of external stereotactic radioablation for the treatment of VT.⁷²

Valvular heart disease

In patients with valvular heart disease (VHD), VA and SCD may occur due to VHD-induced LV dysfunction, hypertrophy, and fibrosis and also due to coexisting triggers (e.g. CAD in elderly patients with aortic stenosis).⁷³ Whether surgical or interventional correction of VHD lowers the risk of SCD remains uncertain although in aortic stenosis the burden of irreversible myocardial fibrosis appears to increase rapidly (with a relative annual progression of mid-wall LGE of 78%) until valve replacement occurs and is closely related to long-term prognosis.⁷⁴ Primary prevention of ICD implantation is indicated for patients who satisfy general guideline-proposed criteria.³ With the exception of mitral valve prolapse, there are currently no solid data on the ability of cardiac imaging to improve risk stratification for VA and SCD in patients with VHD.

Arrhythmogenic mitral valve prolapse and mitral annular disjunction

MVP is characterized by >2 mm displacement of 1 or both mitral valve leaflets above the annulus within the left atrium in end-systole⁷⁵ in the

parasternal or apical long-axis views (*Figure 13*), whilst MAD is defined as a separation between the annulus (i.e. left atrium wall-mitral valve junction) and the LV wall.⁷⁶ CMR is important for confirmation, better visualization of MAD, its location, quantification of MAD length, and, most importantly, detection of associated LGE in the inferolateral wall and in the papillary muscles.⁷⁷ Of note, MAD is a common finding on CMR, and it appears that only inferolateral disjunction warrants consideration of further investigation.⁷⁸

The criteria for primary prevention of ICD implantation in patients with AMVP are not established. Risk markers for severe VA include arrhythmic syncope, frequent PVCs and non-sustained VTs, reduced LVEF, presence of MAD, and papillary muscle or inferolateral LGE.⁷⁷ Reduced LVEF has repeatedly been reported as a risk marker for severe arrhythmic events in patients with AMVP. However, the changes in LV function are often subtle, even occurring within the normal range of LVEF. The presence of LGE is an important risk marker for events, and CMR is useful in patients with MVP and an arrhythmic phenotype.⁷⁷ A recent study showed that CMR T1 mapping was associated with T-wave inversion on the ECG and with VA.⁷⁹ These results indicated that diffuse fibrosis may explain such ECG changes and may be promising for risk stratification in AMVP.

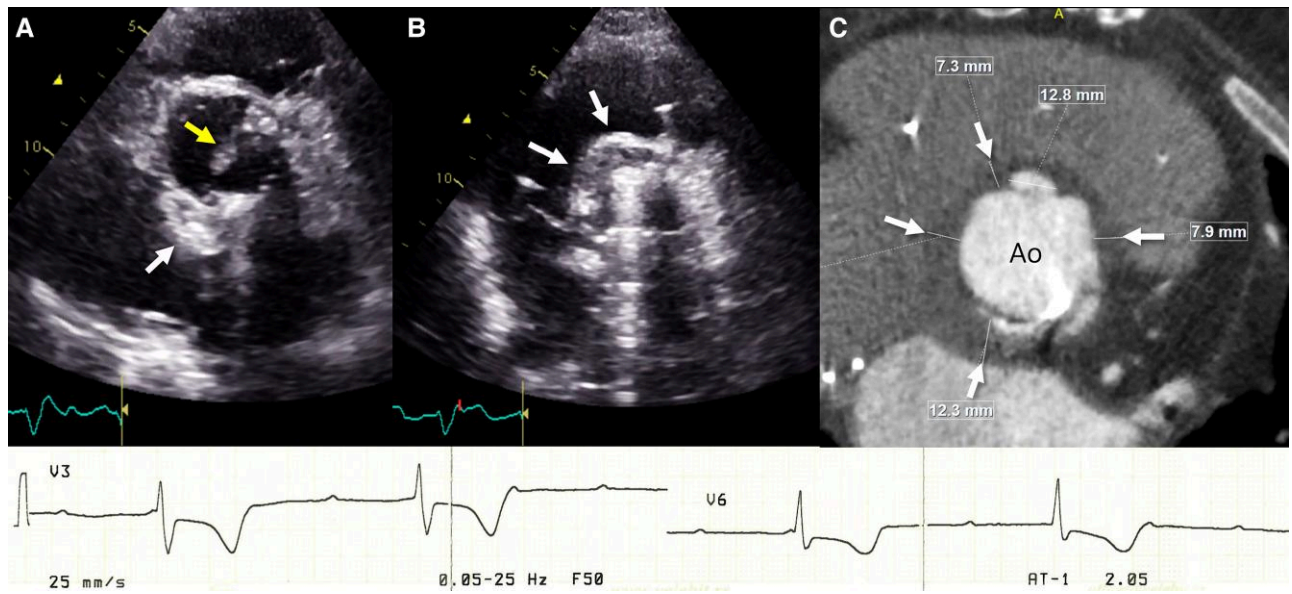


Figure 5 Complete AVB as a consequence of infective endocarditis complicated by an aortic root abscess in a patient with a prosthetic aortic valve. TTE revealed a large vegetation (A, yellow arrow) and aortic root abscess (white arrows, A and B), which was confirmed by CT (C, white arrows). Ao, aorta. CT image courtesy of Radosav Vidakovic, Clinical Hospital Centre Zemun, Serbia.

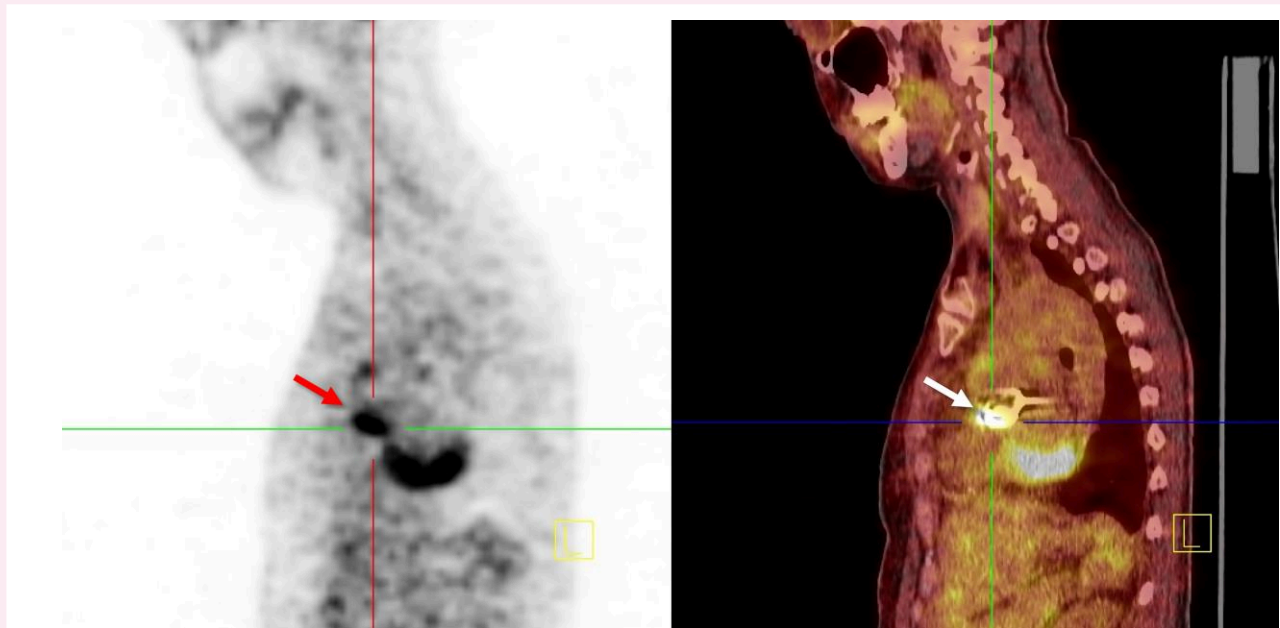


Figure 6 Prosthetic aortic valve endocarditis. Increased focal ^{18}F FDG uptake in the region of prosthetic aortic valve (arrows) on FGD PET (left) and fused PET/CT (right). Image courtesy of Dragana Sobic Saranovic, Center for Nuclear Medicine with PET, University Clinical Center of Serbia.

Inflammatory conditions

It has been shown that the burden, location, and pattern of LGE may improve risk stratification in myocarditis, including amongst patients with preserved LVEF.⁸⁰ Patients with mid-wall anteroseptal LGE have a worse prognosis, in terms of cardiac death, appropriate ICD therapy, resuscitated cardiac arrest, and hospitalization for HF, than those with

other patterns or without LGE.⁸⁰ However, a prognostic threshold for LGE burden has not been defined; moreover, there are no randomized trials showing the superiority of LGE over LVEF to facilitate decision-making for primary prevention of ICD therapy. In patients with cardiac sarcoidosis, LVEF < 35% predicts unfavourable outcomes, but VA can also occur in patients with preserved LVEF.⁸¹ Based on data

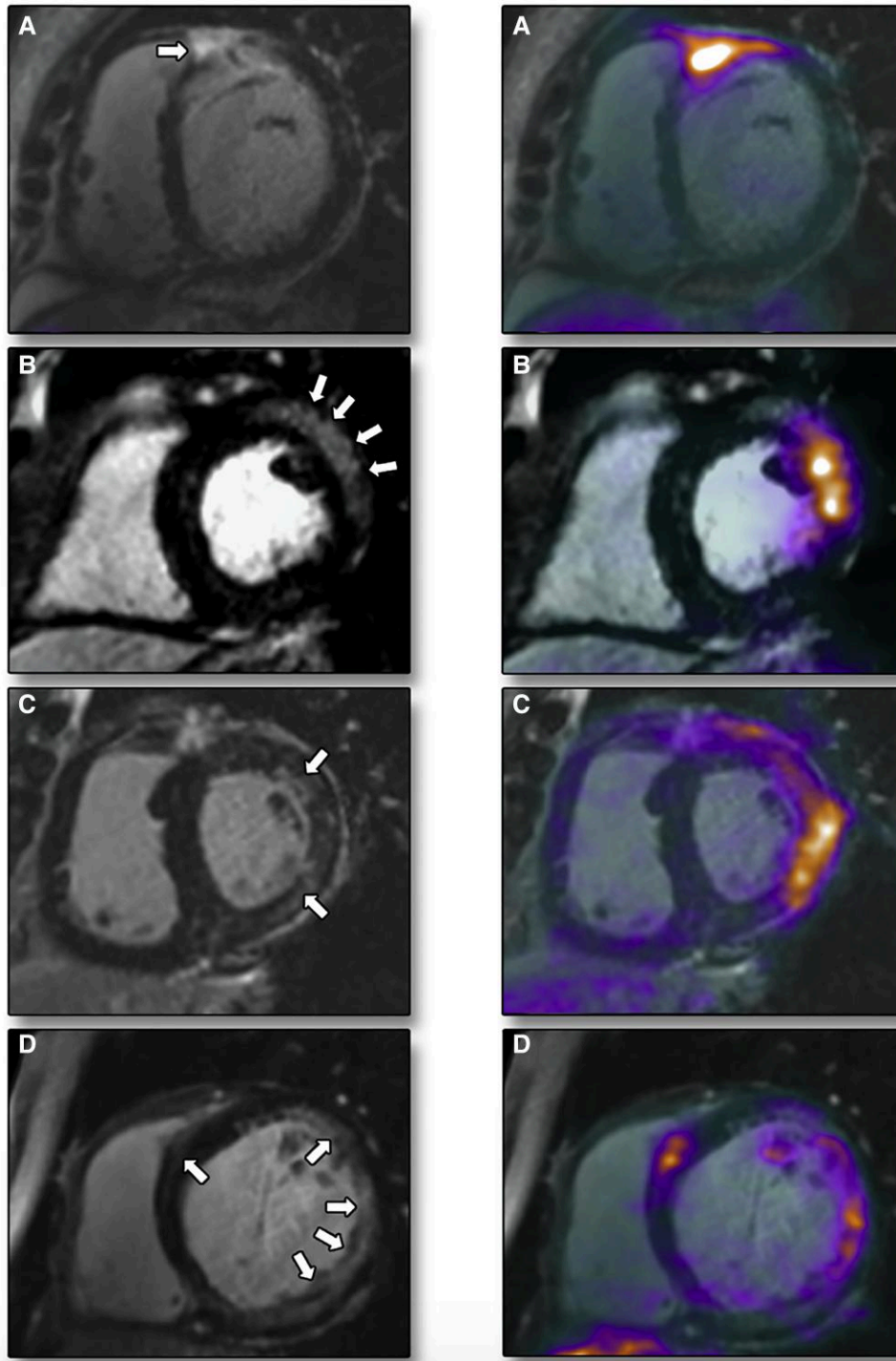


Figure 7 Cardiac sarcoidosis on hybrid cardiac magnetic resonance/PET. LGE CMR images on the left with hybrid ^{18}F FDG CMR/PET images on the right. (A) Subepicardial (near transmural) LGE in the basal anteroseptum extending into the RV free wall with increased FDG uptake localizing to exactly the same region on fused CMR/PET (maximum standardized uptake value = 3.4; maximum tissue-to-background ratio = 2.3; and maximum target-to-normal myocardium ratio = 2.0). (B) Subepicardial LGE in the basal anterolateral wall with increased FDG uptake co-localizing to exactly that region on CMR/PET. (C) Patchy mid-wall LGE in the anterolateral wall with matched increased FDG uptake on CMR/PET. (D) Multi-focal LGE in the lateral wall with matched increased FDG uptake on CMR/PET. Reproduced with permission from Dweck MR et al. *JACC Cardiovasc Imaging*. 2018; 11(1):94–107.

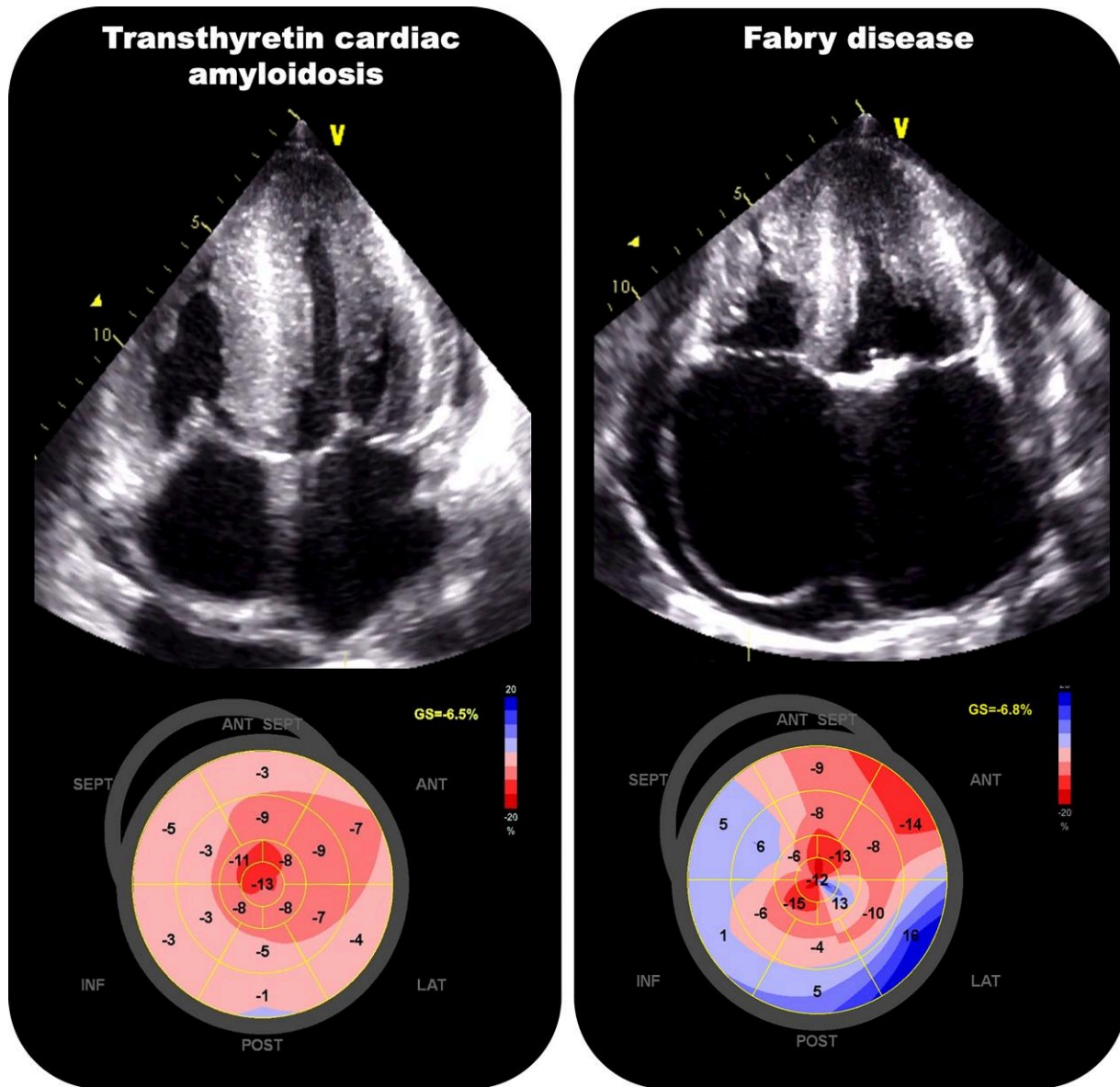


Figure 8 Echocardiographic appearance of transthyretin cardiac amyloidosis and Fabry disease by conventional and speckle-tracking echocardiography. Whilst both diseases belong to the spectrum of hypertrophic phenotype (top panels), the pattern of LV longitudinal strain impairment can be strikingly different (bottom panels). In patients with cardiac amyloidosis, there is an 'apical sparing' or a 'cherry-on-top' pattern on the bull's eye plot of GLS; in patients with Fabry disease, the impairment of longitudinal strain is usually seen at the basal inferolateral LV wall.

demonstrating that patients with LGE had more VA than those without it,⁸² the 2022 ESC guidelines inform that an ICD implantation should be considered in patients with cardiac sarcoidosis who have a LVEF > 35% but significant LGE at CMR after resolution of acute inflammation.³ Whilst the threshold for significant LGE extent was not specified, a recent study suggested that a value of >5.7% had good accuracy for predicting a composite of SCD, significant ventricular VA, and appropriate ICD therapy.⁸³ Also, LGE affecting $\geq 20\%$ of the LV mass has been associated with arrhythmic events in previous reports.^{84,85} A widely accepted definition of significant LGE is not available, partly due to the challenges of precise quantification of LGE burden. In the absence of robust data, it seems prudent to use a lower LGE cut-off (>6%) for the prediction of SCD or VA in patients with cardiac sarcoidosis.^{84,86}

Further studies are needed to refine quantification and to determine the optimal cut-off.

Hypertrophic cardiomyopathy

Imaging is crucial for making a diagnosis of HCM and risk stratification and for decisions on the primary prevention ICDs. According to the ESC guidelines, a complete TTE study and CMR with LGE should be performed in all patients with HCM.^{3,21} Contrast echocardiography, 3DE, and CMR may increase the sensitivity of conventional TTE to detect apical HCM and apical aneurysms⁸⁷ (Figure 14). The ESC HCM risk calculator⁸⁸ is commonly used for estimating individual risk for VA. The parameters in this risk calculator include age, maximum ventricular wall



Figure 9 Bone scintigraphy with ^{99m}Tc -labelled diphosphonates shows no cardiac uptake (A) in a patient without transthyretin amyloidosis (ATTR) and high cardiac uptake (B, arrow) in a patient with ATTR. Image courtesy of Dragana Sobic Saranovic, Center for Nuclear Medicine with PET, University Clinical Center of Serbia.

thickness, left atrial size, maximum LV outflow gradient, family history of SCD, previous non-sustained VT, and unexplained syncope. The prevalence of VA correlates not only with LV wall thickness but also independently with the presence of LGE on CMR.⁸⁹ LGE has not been included in the ESC HCM SCD risk calculator but significant amounts of fibrosis favour ICD implantation.^{3,90,91} According to the 2022 ESC guidelines, in patients with HCM and LV systolic dysfunction (LVEF < 50%), or extensive LGE on CMR (usually defined as $\geq 15\%$ of LV mass) or LV apical aneurysms, ICD should be or may be considered if an estimated 5-year risk of SCD is intermediate or low, respectively.³

Arrhythmogenic RV cardiomyopathy

Imaging has an important role in risk stratification and planning for device implantation. Whilst life-threatening arrhythmias can occur

without overt structural changes in the myocardium,⁹² the presence of structural abnormalities highly increases the risk of VA.^{93–95} RV structural changes, particularly RV dilatation and RV dysfunction, indicate increased arrhythmic risk. According to the 2022 ESC guidelines, in patients with severe RV dysfunction (RV fractional area change $\leq 17\%$ or RVEF $\leq 35\%$), an ICD should be considered.³ Importantly, any LV involvement and dysfunction is associated with increased arrhythmic risk.⁹⁶ In a risk calculation model (arvcrisk.com), only RVEF by CMR was included as an imaging parameter.^{97,98} Two recent papers indicated added prognostic value may be provided by strain echocardiography in these patients.^{95,99}

Unfortunately, inappropriate shocks are frequent in arrhythmogenic RV cardiomyopathy (ARVC) patients, and one-third of patients experience lead-related complications.¹⁰⁰ Special ICD-related concerns in

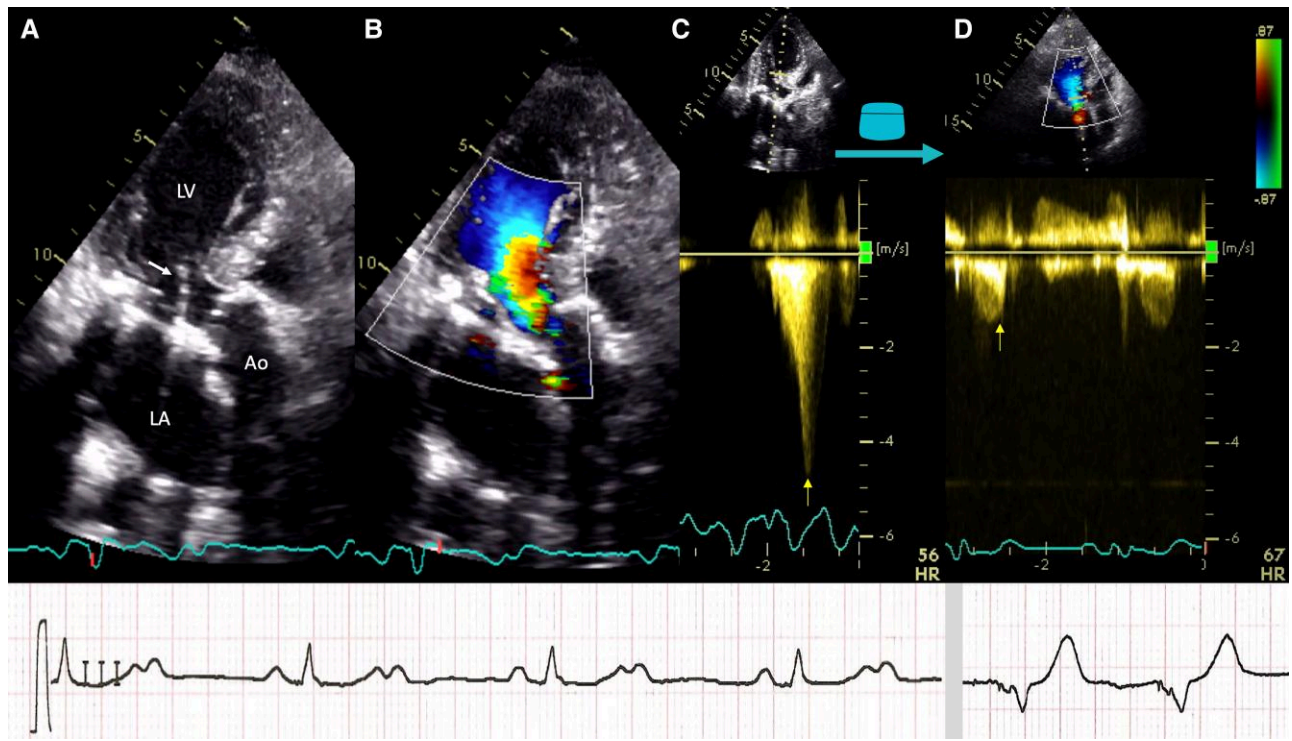


Figure 10 AV sequential pacing in a patient with hypertrophic obstructive cardiomyopathy and a complete heart block. The apical long-axis view shows the systolic anterior motion of the anterior mitral leaflet (A, arrow) causing the LVOT obstruction (B) with a maximum pressure gradient of approximately 80 mmHg (C, arrow). AV sequential pacing with short AV delay resulted in an immediate reduction of LVOT pressure gradient (D, arrow). AV delay was optimized using ECG and TTE. The programmed AV delay was changed gradually until reaching an optimal value with no fusion beats on ECG and no A-wave truncation on the pulsed-wave Doppler of the mitral inflow. Ao, aorta; LA, left atrium; LV, left ventricle.

ARVC, compared with other cardiomyopathies, include the younger age of patients at initial ICD implantation and their higher level of physical activity. Most importantly, there are issues related to electrical contact of the RV lead where areas of fibrosis and poor intra-cardiac signals may be prominent. Low sensing values in the RV may exist already at the time of implantation whilst loss of sense values and increased pacing threshold may also develop over time.¹⁰¹ In a recent study, no non-invasive imaging parameters could predict lead complications.¹⁰⁰

LV hypertrabeculation (LV non-compaction)

Classical clinical manifestations associated with non-compaction include LV dilatation and systolic dysfunction, VAs, and thromboembolic episodes from the spongy LV.¹⁰² Risk stratification for primary prevention ICD follows those for HF.¹⁰³

Lamin A/C cardiomyopathy

Arrhythmic events are frequent in lamin A/C cardiomyopathy and frequently occur before LVEF is severely reduced.¹⁰⁴ LGE on CMR is typically located in the interventricular septum and is probably associated with AV conduction disease.¹⁰⁴ Importantly, patients in need of

pacemaker due to AV block should receive a two-chamber ICD due to the increased risk of VA.³ The 2022 ESC guidelines inform that cardiac resynchronization therapy with defibrillator (CRT-D) should be considered if the patient has AV-block and LVEF < 50% and a high frequency of ventricular pacing is expected.³ When a CRT is indicated for the treatment of HF, patients with lamin A/C cardiomyopathy demonstrate a good response rate to biventricular pacing.¹⁰⁵

Brugada syndrome

Imaging has a limited role in risk stratification and device implantation in patients with Brugada syndrome. However, there are preclinical reports and clinical case studies indicating a potential overlap between ARVC and Brugada syndrome, with the RVOT area as a common region of arrhythmogenicity.^{106–108} A recent study confirmed that a dilated RVOT was associated with VA on top of a spontaneous Brugada type 1 ECG pattern.¹⁰⁶ By contrast, a normal RVOT diameter (<32 mm or indexed RVOT diameter of <18 mm/m²) was associated with the absence of arrhythmic events in patients with Brugada syndrome with a spontaneous type 1 ECG and previous syncope.¹⁰⁸ These findings may indicate a possible clinical value of repeated imaging assessments in risk stratification for VAs.

Clinical advice

Cardiac imaging reports in patients with HCM must contain parameters included in the ESC risk calculator: maximum wall thickness, maximum LVOT pressure gradient, and LA diameter.



CMR LGE is useful to help decision-making regarding primary prevention ICDs in patients with HCM at intermediate and low risk.



CMR is useful to help risk stratification in patients with MVP/MAD and an arrhythmic phenotype.



Assessing RV structure and function by CMR in patients with arrhythmogenic cardiomyopathy is useful for risk assessment and selection for primary prevention ICDs.



In patients with cardiac sarcoidosis and LVEF > 35%, myocardial scar assessment by CMR or PET is useful to improve risk stratification of VA and SCD and selection of patients for primary prevention ICDs.



Imaging of patients undergoing CRT

CRT is an established therapy for patients with HF, reduced LVEF, and a wide QRS complex who remain symptomatic despite optimal medical treatment.¹⁰³ Unfortunately, the rate of patients without volumetric response to CRT remains stable in the range of 30–40% despite technical improvements and accumulating experience.¹⁰⁹ Current selection criteria are based on patient symptoms, QRS width and morphology, and LVEF.^{2,103} In the 2010 focused update of the ESC guidelines on device therapy in HF, mechanical dyssynchrony, assessed by time-to-peak velocity parameters, was considered a useful tool for CRT patient selection in subgroups less likely to respond to this treatment (e.g. a QRS width of 120–150 ms).¹¹⁰ However, its use has been refuted by the disappointing results of a multi-centre, observational study that questioned both the accuracy and reproducibility of this approach.¹¹¹ Furthermore, in the subsequent Echo-CRT randomized controlled trial, mechanical dyssynchrony-driven CRT implantation not only failed to reduce the rate of death or hospitalization for HF but also might even have increased mortality in patients with narrow QRS complexes.¹¹² Over the past decade, the superiority of novel approaches for mechanical dyssynchrony assessment over time-to-peak parameters and their favourable association with CRT outcome has been repeatedly shown in observational studies.^{113–117} However, guideline recommendations for CRT patient selection are not likely to be refined before the accuracy and reproducibility of novel parameters are supported by evidence from randomized controlled trials. Finally, the response to CRT is no longer considered a binary variable, since patients who either improve or stabilize after CRT fare better than those with disease progression despite CRT.^{118–121}

In the following section, we discuss all potentially useful imaging parameters, acknowledging that several are beyond current guideline criteria and also revisit the relationship of different response metrics with patient outcomes after CRT.

Assessment of the mechanical consequences of conduction delays

AV dyssynchrony

Prolonged AV conduction can lead to impaired LV diastolic filling and thereby reduced LV preload and stroke volume. This type of dyssynchrony can be assessed with pulsed-wave Doppler echocardiographic recordings of the mitral valve inflow, typically characterized by reduced LV filling time leading to fusion of the early (E) and late (A) diastolic waves (Figure 15), which nevertheless is also favoured by higher heart rate in normal individuals. An LV filling time < 40% of the total cardiac length denotes significant AV dyssynchrony.¹²² CRT allows control of the AV interplay that contributes in part to the favourable effects of CRT via improved AV coupling¹²³ and also allows optimal beta-blocker treatment whilst avoiding AV block. Of note, the AV delay can also be programmed in dual-chamber pacing.

Interventricular dyssynchrony

The time difference between RV and LV ejection defines interventricular mechanical dyssynchrony and can be determined from pulsed-wave Doppler traces as the time elapsed between the onset of flow in the RVOT and LVOT (Figure 15). A time delay of >40 ms is considered a significant interventricular mechanical delay but does not predict CRT response with sufficient accuracy for clinical use.¹¹¹

Intraventricular dyssynchrony

Intraventricular dyssynchrony refers to the dyssynchronous motion or deformation of the different regions of the LV. Alternatively, the term 'LV mechanical dyssynchrony' is used to distinguish it from the electrical phenomena seen on the ECG. Intraventricular dyssynchrony is not well defined and many, mainly echocardiographic parameters have been proposed for its measurement. Early dyssynchrony parameters were mostly based on time-to-peak tissue velocity or strain measurements and could sensitively detect mechanical dyssynchronization amongst the different regions of the LV and were therefore sensitive criteria for the detection of LV mechanical dyssynchrony.^{124–127} However, time-to-peak measurements demonstrated poor specificity¹²⁸ and therefore failed to selectively identify patients who would benefit from CRT and did not provide added value beyond established guideline criteria.^{111,112} In order to improve patient selection by cardiac imaging, it is therefore important to find selection criteria that are not only sensitive but also specific and to identify motion or deformation patterns that are amenable to CRT (Figure 16).

Intraventricular dyssynchrony amenable to resynchronization

Typical LBBB causes early activation of the septum and delayed activation of the lateral wall (Figure 16). The septal activation ends diastole when the cavity pressure and the load on the septal myocardium are low. The delayed contraction of the lateral wall then bears the main work load of systolic ejection whilst the septum is stretched (Figure 16). The septal stretching can be observed as a short 'notching' in the strain curve of a still functioning septum in early stages of cardiomyopathy but may become holosystolic when the septum is thin and weak in more advanced states of LV remodelling.^{129,130} In animal models, the imbalance in loading of the septum and lateral wall has been shown to lead to progressive atrophy of the septum, hypertrophy of the lateral wall, and dilatation of the LV,^{131,132} changes that can also be observed in patients.¹³¹ Furthermore, the uncoordinated contraction and relaxation pattern of the LV myocardium causes a slower LV pressure rise and decay and hence longer isovolumic contraction and relaxation times, respectively. As a consequence, LBBB shortens LV filling time and impairs LV function in a similar way as described above for AV dyssynchrony (Figure 15).

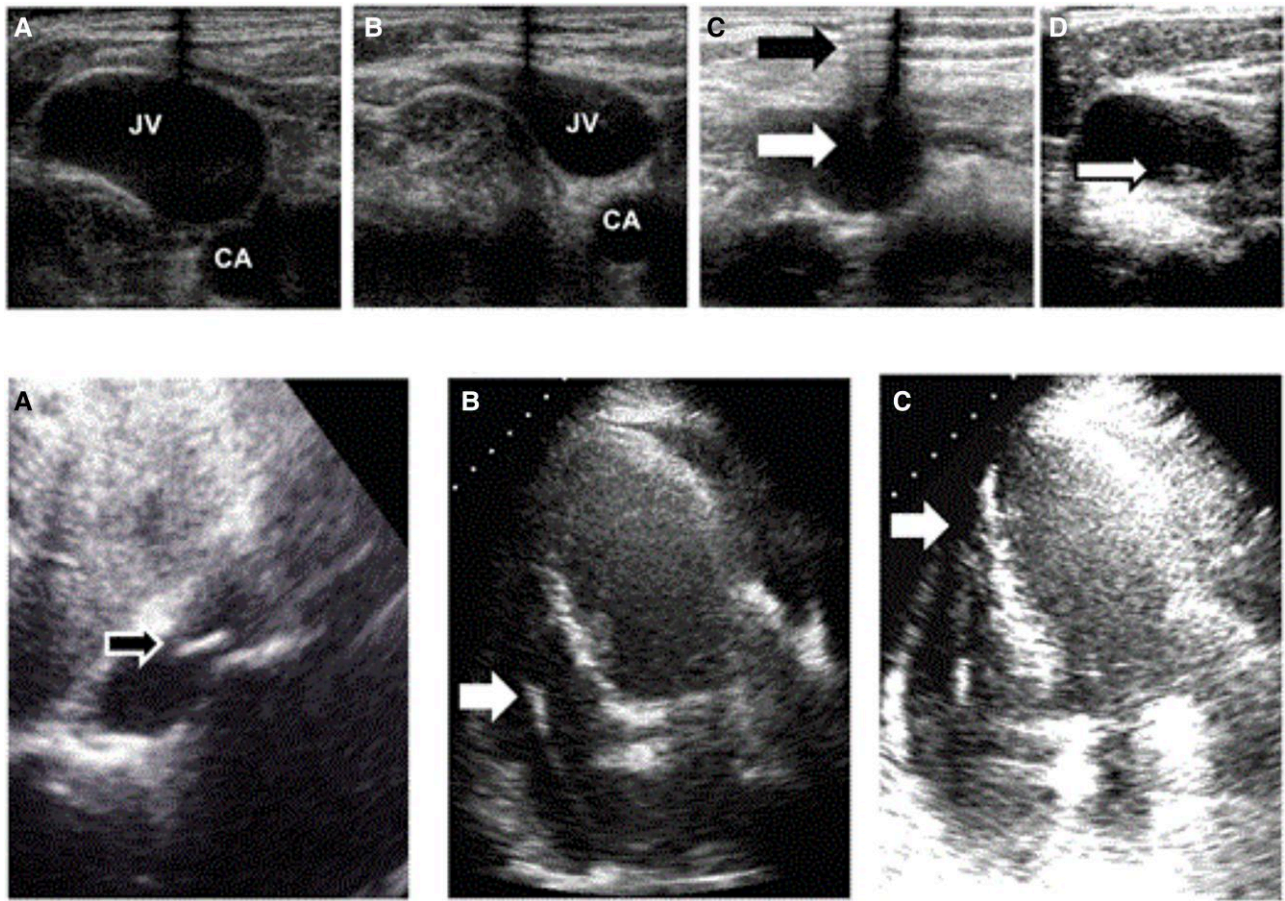


Figure 11 Ultrasound-guided jugular vein puncture and placement of the pacing electrode. Top panels: (A) Echographic identification of the internal jugular vein (JV) and carotid artery (CA). (B) Compressibility confirms the venous nature of the vessel identified (C) Echography-guided puncture of the internal jugular vein (black arrow: needle pathway; white arrow: needle tip). Using the Seldinger technique, a guidewire is advanced through the needle: echocardiographic guidance confirms the correct position of the wire in the internal jugular vein lumen (short axis view shown in D). Bottom panels: After identification of the electrode tip in the right atrium (A), the pacemaker is advanced in the RV after crossing the TV (B). The lead pathway to the RV apex is monitored under echocardiographic guidance (C). Reproduced and modified with permission from Ferri LA *et al. Eur Heart J Acute Cardiovasc Care.* 2016; 5(2):125–9.

Regional LV deformation patterns in LBBB have to be distinguished from those caused by myocardial ischaemia or scar. In ischaemic and scarred myocardium, a reduced shortening in systole and a delayed shortening peak after aortic valve closure (post-systolic shortening) are common findings.¹³³ If only the temporal occurrence of myocardial deformation peaks is considered, a ventricle with scar shows a 'dispersion' of shortening peaks across affected segments that are not recruitable and cannot be therefore resynchronized (Figure 17). LV dispersion has been shown to be related to the risk of life-threatening arrhythmia.⁶¹ However, mechanical dispersion should not be used in the context of dyssynchrony assessments, since it is sensitive to both ischaemic and conduction disease substrates.¹³⁴

In ischaemic cardiomyopathy with conduction delay, the typical LBBB pattern of intraventricular dyssynchrony may be complicated by regional dysfunction due to scar.¹³⁵ Such hearts show a mechanical dyssynchrony, but not all patterns of dyssynchrony may be improved by CRT. It is therefore of utmost importance that imaging parameters used to identify potential CRT responders are specific enough to identify dyssynchrony patterns that are amenable by CRT.¹¹³ Several novel parameters of mechanical dyssynchrony have been successfully tested

in observational studies,^{114–116} but all are lacking supportive evidence from prospective, randomized trials. Mechanical dyssynchrony as a selection criterion for CRT is currently being tested in the ongoing randomized AMEND-CRT trial (ClinicalTrials.gov Identifier: NCT04225520).

Other imaging modalities to detect LV mechanical dyssynchrony

In theory, any imaging modality with sufficient temporal and spatial resolution may be used to identify the typical deformation patterns described above. Modern 3D echocardiography can reach a sufficient temporal resolution and can provide time-aligned information on the deformation of all segments of the LV within one acquisition. Obtaining speckle-tracking echocardiographic 3D data sets with good regional quality, however, is challenging and has low feasibility and reproducibility and, in its current form, limited added value over 2D approaches.¹³⁶ CMR sequences with sufficient frame rate are available and tracking methods can be applied similar to echocardiographic images. However, regional tracking with CMR demonstrates poor reproducibility and must be used with caution.^{137,138} Radial tracking,

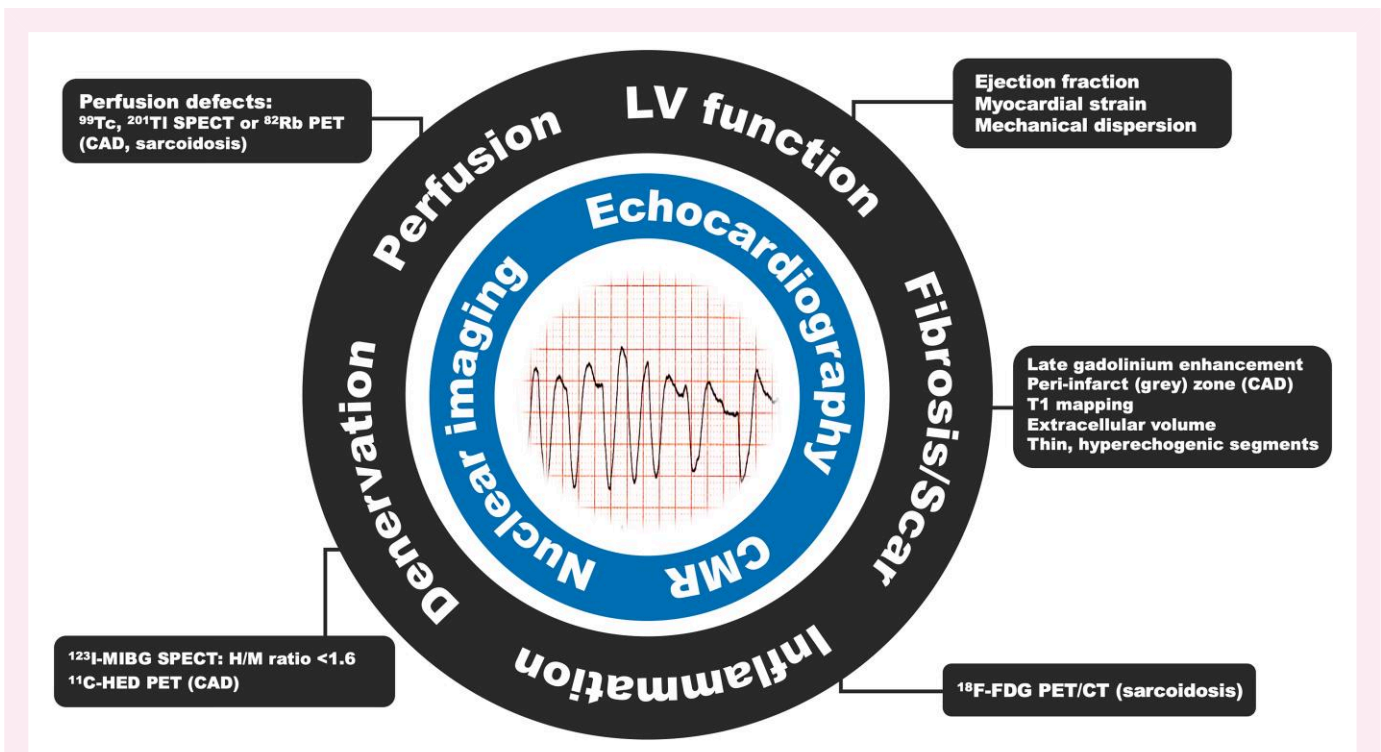


Figure 12 Multi-modality imaging for the identification of tissue characteristics that can be associated with ventricular arrhythmia. ^{11}C 11-HED, 11-carbon-meta-hydroxyephedrine; CAD, coronary artery disease; CMR, cardiovascular magnetic resonance; CT, computed tomography; ^{18}F -FDG, 18-fluorodeoxyglucose; H/M, heart-to-mediastinum ratio; ^{123}I -MIBG, 123-iodine-labelled meta-iodobenzylguanidine; LV, left ventricle; PET, positron emission tomography; Rb, rubidium; SPECT, single-photon emission computed tomography; Tc, technetium; Tl, thallium.

tagging approaches, and velocity-encoded imaging sequences may provide better results but require cumbersome post-processing. CT data, when acquired throughout the entire cardiac cycle with ECG-tagging, may also have sufficient temporal and spatial resolution to assess LV dyssynchrony,¹³⁹ but with the disadvantage of ionizing radiation. Whilst scintigraphic methods have limited temporal and spatial resolution, they can provide dyssynchrony information through analysis of the amplitude (reflecting wall thickening) and phase (reflecting the timing of regional wall motion) of tracer uptake. Studies have suggested the use of the standard deviation of phase-related parameters as a potential criterion.^{140,141} Of note, scintigraphy also has the disadvantage of ionizing radiation.

Assessment of HF aetiology

Current ESC guidelines² give common recommendations for CRT implantation regardless of HF aetiology, since randomized clinical trials showed similar benefit in terms of mortality and HF hospitalizations between patients with ischaemic or non-ischaemic HF. However, the same ESC guidelines recognize that patients with an ischaemic aetiology have less improvement in LV function after CRT, probably due to presence of myocardial scar tissue, which is less likely to be associated with favourable remodelling. Nonetheless, guideline-proposed recommendations to consider implantation of CRT-D rather than CRT with pacemaker (CRT-P) are based on individual risk assessment that includes, amongst other factors, ischaemic aetiology of HF and the presence of myocardial fibrosis.² Echocardiography represents the first-line imaging modality for the characterization of LV function and may give important suggestions regarding HF aetiology. However, CMR with LGE is considered the reference standard assessment of cardiac structure and function as well as uniquely providing information on myocardial scar

pattern, extent, and location. Such scar is typically subendocardial or transmural in patients with ischaemic heart disease, as compared with the mid-wall or subepicardial scar in patients with non-ischaemic cardiomyopathy. In a prospective, observational study, pre-implantation scar assessment by CMR was predictive of appropriate ICD therapies and SCD in CRT patients¹⁴² whilst data from randomized studies are currently lacking.

Pre-implantation stress imaging (including echocardiography and nuclear or CMR perfusion imaging) may be used for the assessment of inducible ischaemia and viability in those being considered for coronary revascularization. The integrated use of different imaging modalities may therefore help optimize patient selection for CRT and maximize cost-effectiveness.

Assessment of scar burden and localization

Approximately half of patients referred for CRT have an ischaemic aetiology of HF. The presence, location, and extent of scar tissue determine response to CRT. Lateral scar is an impediment for efficient LV free wall pacing. It reduces CRT response and increases the risk of HF, hospitalization, and death.^{143,144} When analysing mechanical dyssynchrony in patients with LBBB, lateral scar leads to pseudo-normalization of septal deformation patterns.¹³⁵ Septal strain curves therefore always need to be interpreted in the context of the lateral curves.¹³⁵ Septal scar reduces the chances of septal functional recovery and can therefore also be detrimental to successful CRT.¹⁴⁵ LV lead deployment over non-scarred myocardium, as assessed by LGE-CMR, was associated with a higher percentage of LV reverse remodelling and better clinical outcomes after CRT.^{146,147} However, randomized trials have not

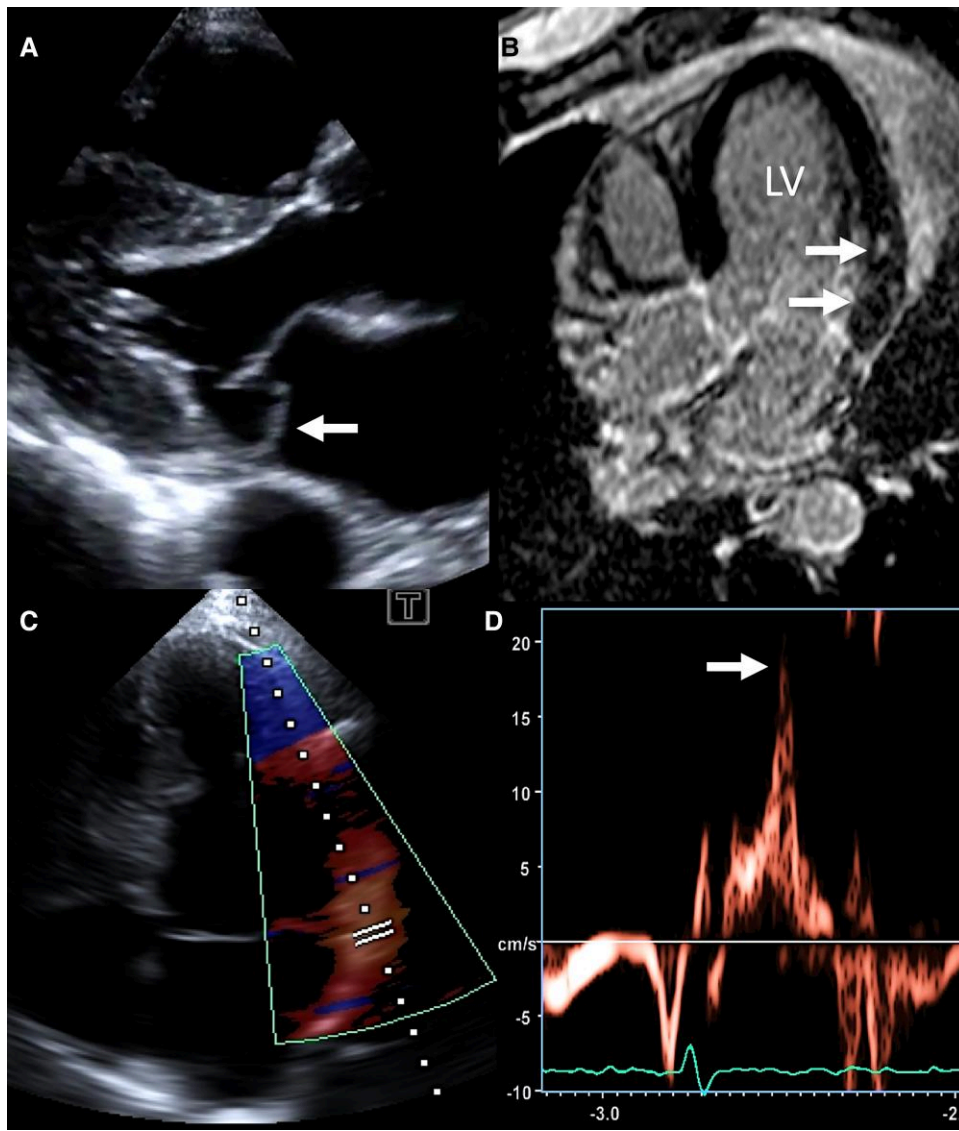


Figure 13 Echocardiography and cardiovascular magnetic resonance imaging in arrhythmogenic mitral valve prolapse. (A) The parasternal long-axis view showing a prolapse of the posterior mitral valve leaflet (arrow). (B) LGE in the anterolateral LV wall (arrows). (C and D) A late systolic spike (D, arrow) in the lateral mitral annular tissue Doppler velocity signal ('Pickelhaube sign'). CMR image courtesy of Predrag Milicevic, Clinical Hospital Centre Zemun, Belgrade, Serbia.

unequivocally demonstrated that the guidance of LV lead implantation based on imaging (assessing myocardial scar or site of latest mechanical activation) is superior to an electrically guided CRT strategy.^{2,148,149}

Perfusion defects at rest on SPECT or PET generally indicate the presence of scar tissue. However, in the presence of dyssynchrony, reduced septal tracer uptake may also be caused by partial volume effects in the thinned septum and the lower work and reduced metabolism in this LV region. The extensive LV contraction abnormalities induced by LBBB cause regional myocardial metabolic and structural remodelling, even in the absence of reductions in blood flow. Therefore, reduced septal tracer uptake does not necessarily indicate scar, and the accuracy of nuclear methods to identify scar tissue is reduced in patients with LV dyssynchrony (Figure 18).^{150,151} However, a matched perfusion/metabolism defect on PET imaging can detect true scar in patient with LBBB.¹⁵²

Response to CRT

Definitions of response

Favourable effects of CRT can be observed immediately as well as over the mid and the long terms (Table 4).

Correction of conduction abnormality can immediately translate into favourable haemodynamic changes such as increases in blood pressure, cardiac output, dP/dt , and LV filling period and decreases in mitral regurgitation (MR) and signs of dyssynchrony.^{116,153} Mid- to long-term effects of successful resynchronization include LV reverse remodelling,^{154,155} decreased MR,¹⁵⁶ increased EF, improved LV diastolic function,¹⁵⁷ LA function,¹⁵⁸ and RV function,¹⁵⁹ as well as reductions in both VA^{154,160} and atrial fibrillation.¹⁵⁸ Overall, these effects improve the well-being and functional capacity of patients and reduce the need for diuretics, the rate of recurrent hospitalizations, cardiac, and overall mortality.

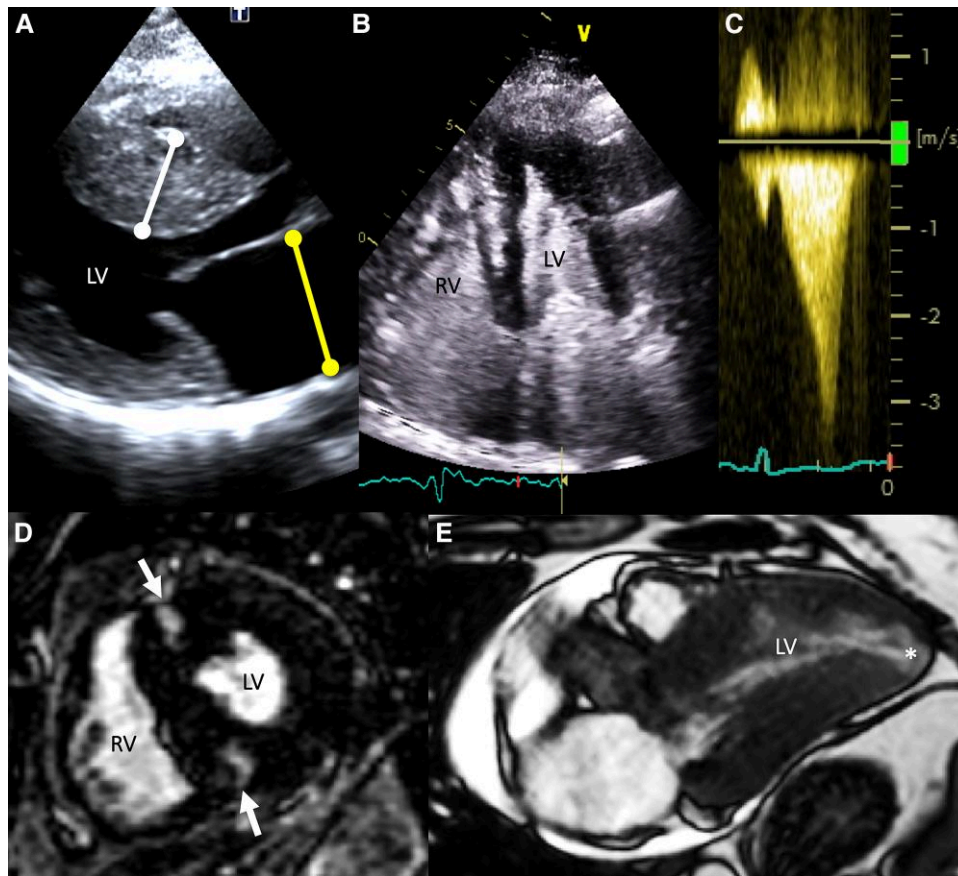


Figure 14 Echocardiography and cardiovascular magnetic resonance imaging in HCM. (A) Prominent septal hypertrophy (white line) and dilated left atrium (yellow line). (B) Contrast echocardiography for the detection of apical hypertrophy. (C) Typical late-peaking, dagger-shaped appearance of continuous-wave Doppler signal in a patient with LVOT obstruction. (D) LGE (arrows) at the RV insertion points in a patient with symmetric HCM. (E) The asterisk (*) indicates an apical LV aneurysm in a patient with HCM and mid-ventricular obstruction. HCM, hypertrophic cardiomyopathy; LV, left ventricle; RV, right ventricle. CMR images courtesy of Predrag Milicevic, Clinical Hospital Centre Zemun, Belgrade, Serbia.

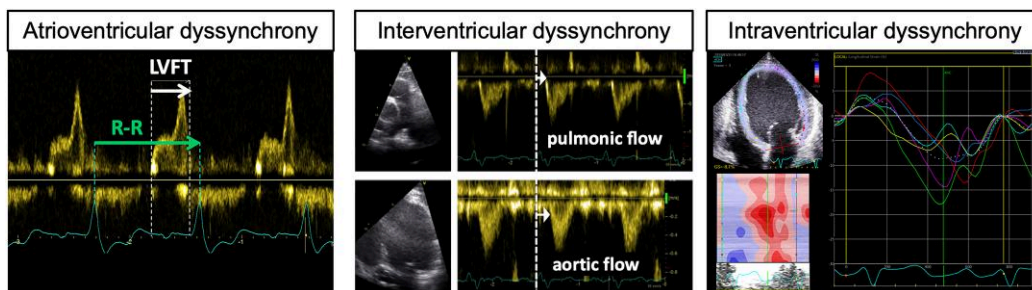


Figure 15 Echocardiographic assessment of mechanical dyssynchrony. Electrical AV and ventricular conduction delays are visible as prolonged PQ interval or abnormal QRS morphology and width on ECG and result in different mechanical phenomena. Left: prolonged AV conduction may result in a fusion of E and A waves and a reduced LV filling time (LVFT) on transmitral pulsed-wave Doppler measurements. Middle: LBBB causes interventricular dyssynchrony that can be assessed as time delay between the onset of right and LV ejection on pulsed-wave Doppler recordings of RVOT and LVOT. Right: prolonged intra-ventricular conduction can be also reflected by mechanical events in the LV, which can be assessed by speckle-tracking echocardiography (here, septal and lateral strain curves are shown).

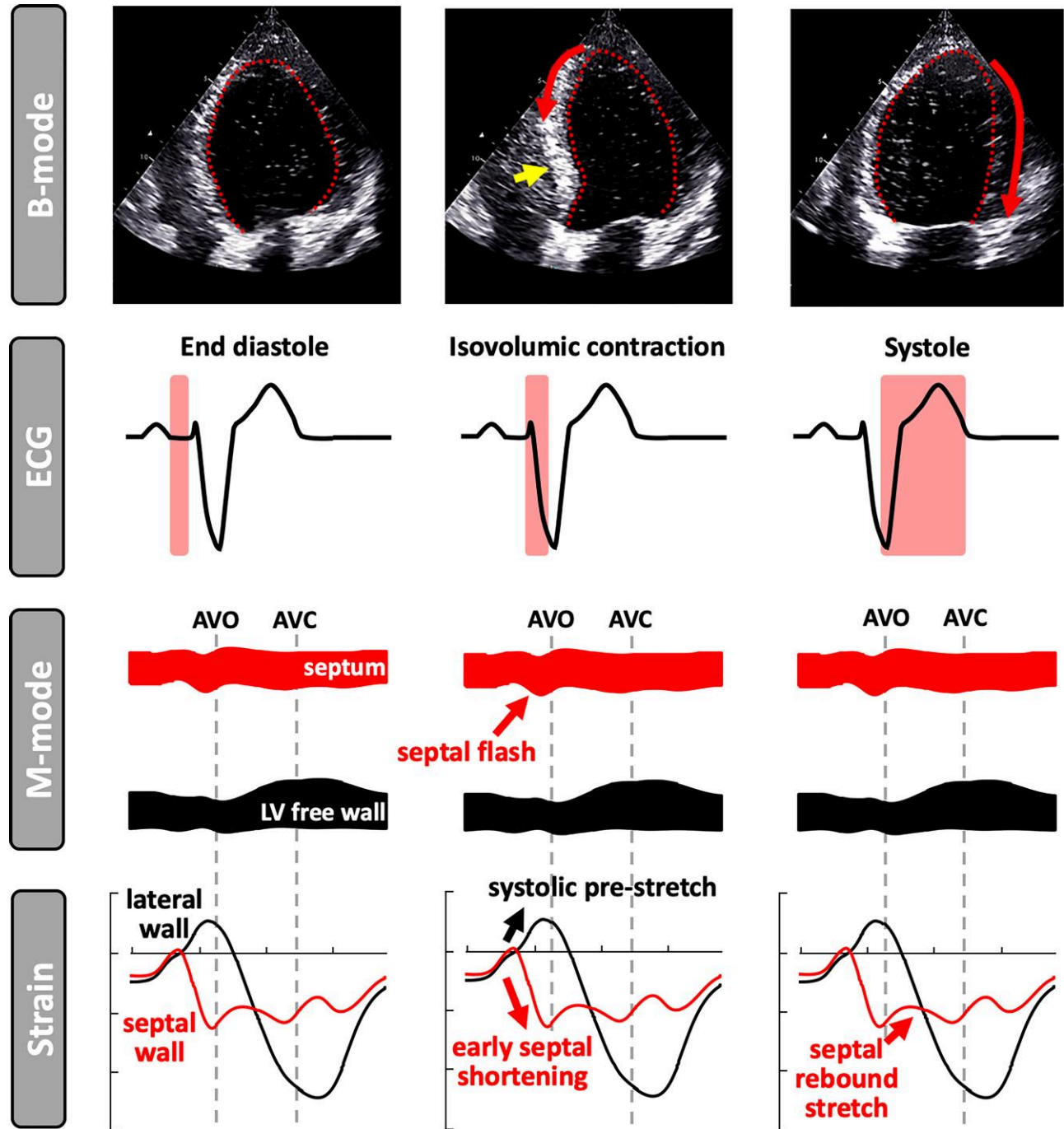


Figure 16 The typical sequence of mechanical and electrical events in LBBB on B-mode, M-mode and strain echocardiography. An early electrical activation of the septum results in a short initial septal contraction and causes the apex to move septally, whilst the septum moves leftward (yellow arrow in B-mode, red arrow in M-mode, and red strain curve). The delayed activation of the lateral wall pulls then the apex laterally during the ejection phase whilst stretching the septum (red arrow in B-mode and black in strain curve). This typical sequence of the septal-to-lateral apex motion is described as ‘apical rocking’. The septal inward motion is described as ‘septal flash’. Modified with permission from Stankovic I et al. *Eur Heart J Cardiovasc Imaging*. 2016; 17(3):262–9 (upper two panels).

CRT response rate is however challenging to assess and varies significantly based on the definition of response and which of the above parameters are included.^{161,162} Response rate based on clinical endpoints (such as New York Heart Association class or quality of life scores) is higher than the response rate based on LV reverse remodelling

assessed by imaging.¹⁶³ Changes in echocardiographic markers of reverse remodelling remain the most commonly used surrogate endpoints of CRT response.¹⁵⁵ LV reverse remodelling is usually defined by a decrease in end-systolic volume (ESV) of >15% compared with baseline or by an absolute increase in LVEF of >5–10%. On this basis,

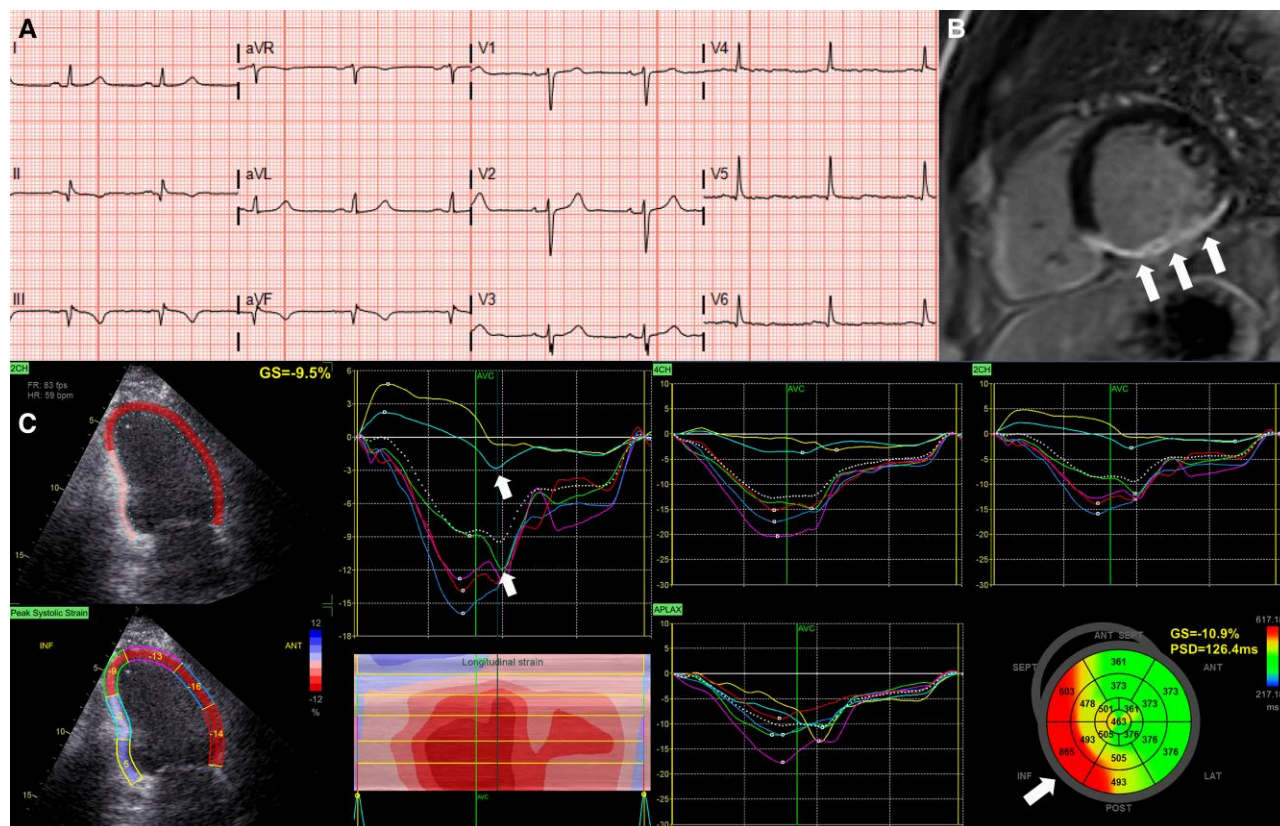


Figure 17 Regional myocardial deformation patterns in ischaemic myocardium. (A) Electrocardiogram of a patient with inferior and inferolateral infarction. (B) LGE showing transmural scar in the inferior septum, inferior, and inferolateral wall of the LV. (C) Echocardiographic assessment of the same patient by speckle-tracking-based strain. Myocardial scar causes systolic lengthening and a pronounced post-systolic shortening (arrow) in the affected segments. Furthermore, peak myocardial deformation occurs at different points in time ('dispersion'). LV myocardial dispersion can be quantified by calculating the standard deviation of the segmental time-to-peak values (bull's eye at the lower right indicating with red and yellow colours the segments with the most pronounced post-systolic shortening). PSD, peak strain dispersion.

non-response has been detected in 30–40% of patients.^{155,161,163} However, the agreement between improved patient functional status and these markers of reverse remodelling is only modest.^{161,164,165} Reverse remodelling most likely translates into favourable outcomes, but lack of reverse remodelling is not equivalent to non-response in all patients.^{118,119} In some patients, LV volume 'stabilization' (i.e. no further volume expansion) after CRT may already be a favourable effect providing a survival benefit^{165–167} as many assumed non-responders demonstrate a deterioration in cardiac performance when their device is switched off¹²⁰ (Figure 19). In addition, repeat echocardiography is not well suited to detecting more subtle changes in cardiac structure and function due to the inherent variability in echocardiographic biplane volume measurements. Furthermore, it remains difficult to define the optimal time point at which to evaluate the response to treatment, given the continuous remodelling and dynamic nature of HF.¹⁶⁶ In the recent ADVANCE CRT registry, recurrence of clinical HF was a stronger marker of a poor prognosis than a lack of echocardiographic reverse remodelling amongst patients with LBBB receiving CRT.¹⁶⁷ From that perspective, it is challenging to dichotomize response to CRT using LV reverse remodelling or any other standalone marker as a surrogate of clinical outcome.

Composite clinical scores (CCS) may be a more appropriate tool to evaluate the effect of CRT^{118,121,168} because slowing down the progression of the disease is a positive outcome and is not necessarily

associated with reverse remodelling. This is particularly evident in patients with ischaemic cardiomyopathy who manifest less reverse remodelling but demonstrate a similar risk reduction after CRT for HF admissions and death as the non-ischaemic group.¹⁶⁹

In a subset of patients, super-response is observed. This is usually defined as LVEF increase above 50% together with a decrease in ESV of >15%, although a universal definition of super-response to CRT does not exist. Independent of the definition, however, super-responders with pronounced LV reverse remodelling do demonstrate superior clinical outcomes.^{160,170}

Imaging predictors of response

Several imaging parameters have been developed recently to predict response to CRT.^{114,115,171} Accumulated evidence from several non-randomized studies suggests that these parameters, discussed below, could be a useful addition for CRT patient selection.

Visual echocardiographic analysis

Early activation of the septum in LBBB causes a short and rapid inward motion of the septum that is commonly referred to as 'septal flash' (Figure 16).¹⁷¹ Septal flash is a very sensitive parameter but may lack some specificity as it may appear even if relevant parts of the septum are ischaemic scar. Nevertheless, it has been shown to identify CRT

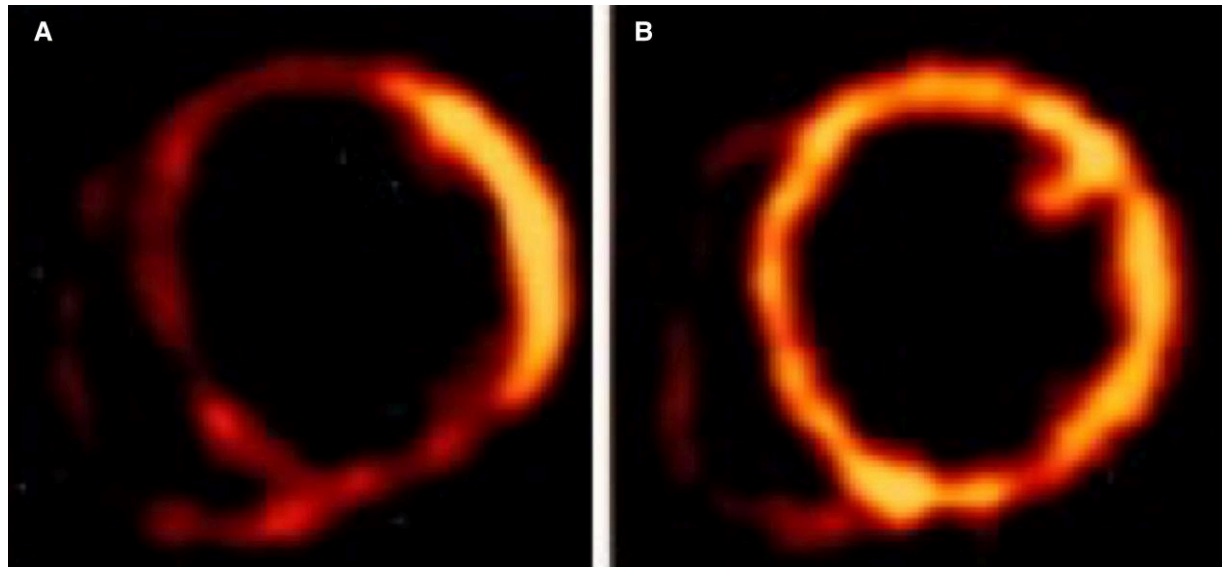


Figure 18 Scintigraphy with reduced septal tracer uptake in LBBB. LBBB causes underuse of the early activated septum with thinning of the LV wall and low regional work performed, as well as a thickened lateral wall with a high workload. In PET images, this leads to a reduced tracer uptake in the septum and high uptake values in the lateral wall, indicating LBBB-induced regional myocardial metabolic remodelling. (A) A fluorodeoxyglucose-PET in a 50-year-old female with LBBB. (B) Same patient after resynchronization therapy, showing metabolic homogeneous uptake in the septum vs. lateral wall. Modified with permission from Nowak B *et al.* *J Am Coll Cardiol.* 2003; 41(9):1523–8.

Table 4 The spectrum of response to CRT

Immediate/short-term response

- Coordination of contraction
- Decrease in mitral regurgitation
- Increase in diastolic filling and cardiac output

Mid- to long-term response

- Increase in end organ perfusion, decrease in sympathetic and RAAS activity
- Increase in myocardial perfusion
- Decrease in ventricular volumes
- Decrease in mitral regurgitation
- Increase in LVEF and RV function
- Decrease in ventricular arrhythmias and atrial fibrillation
- Increase in functional capacity and well-being
- Decrease in heart failure hospitalizations
- Decrease in cardiovascular and all-cause mortality

LVEF, left ventricular ejection fraction; RAAS, renin–angiotensin–aldosterone system; RV, right ventricular.

responders with good accuracy.^{114,171} A low dose dobutamine challenge increases mechanical dyssynchrony and can help to unmask septal flash in a minority of difficult cases.^{172,173} ‘Apical rocking’ describes the typical LV motion pattern caused by LBBB conduction delay. Early septal contraction at end-diastole pulls the LV apex towards the septum, whilst lateral wall contraction then causes pronounced lateral motion of the apex during the ejection phase.¹⁷⁴ Detecting this apical rocking pattern has been demonstrated in several studies to be both sensitive and specific for CRT

response and strongly associated with successful outcome after CRT.^{114,175} Apical rocking is also related to favourable outcome in patients undergoing upgrade from regular pacing to CRT and in CRT recipients with a QRS < 150 ms.^{114,176} Apical rocking is diminished in the presence of scar, which is advantageous in the assessment of CRT candidates with ischaemic cardiomyopathy.¹⁴⁵ Both septal flash and apical rocking are relatively simple markers that can be obtained by visual inspection of routine 2D cine-loops and do not require any further quantitative off-line analysis. These visual phenomena are consistent with studies of more quantitative measures of systolic stretch by strain imaging and likely relate to the same electromechanical pathophysiology (Figure 16).

Quantitative echocardiographic analysis of the LV

Echocardiographic strain imaging enables quantification of LV segmental deformation and is therefore a useful aid for the analysis of global as well as regional LV mechanical function. An increased baseline value of absolute GLS, an integral measure of apex-to-base myocardial deformation, has been shown to be strongly associated with LV reverse remodelling and clinical outcome after CRT.^{116,177}

Several studies have analysed septal strain patterns as predictors for CRT response.^{129,178,179} In early disease, the delayed lateral wall contraction causes a short ‘notching’ in the septal strain curve, whilst in advanced disease, the septum shows systolic stretching (Figure 16). It has recently been suggested that systolic septal stretching increases over time, reflecting LBBB-induced ventricular remodelling.¹³⁰ This may explain why dyssynchrony indices incorporating septal stretch are sensitive and specific for volumetric response and strongly associated with clinical outcome after CRT.^{116,133,178–180}

More recently, the calculation of segmental myocardial work has been suggested. For this, segmental pressure-strain (or stress-strain) loops are constructed utilizing echocardiographic speckle-tracking strain and an estimate of the LV pressure¹⁸¹ (Figure 20). Regional work distribution is associated with LV remodelling in LBBB¹³² and reverse



Figure 19 Patient with ischaemic dilated cardiomyopathy deemed volumetric non-responder 9 months after CRT. Haemodynamic deterioration is evident with the first beat as the CRT is turned off (red arrow). dP/dt , delta pressure/delta time; EKG, electrocardiogram; LV, left ventricle; LVOT, left ventricular outflow tract; TVI, time velocity integral.

remodelling after CRT implantation¹⁸² and has been suggested as a predictor of CRT response.^{183,184} In a recent observational prospective multi-centre trial, the LV lateral wall to septal work difference as a single parameter proved to have similarly good predictive value as

visual analysis by septal flash and apical rocking.¹¹⁵ When either method is combined with assessment of septal scar by CMR, CRT response is predicted with significantly higher accuracy than the former approaches alone.^{115,185}

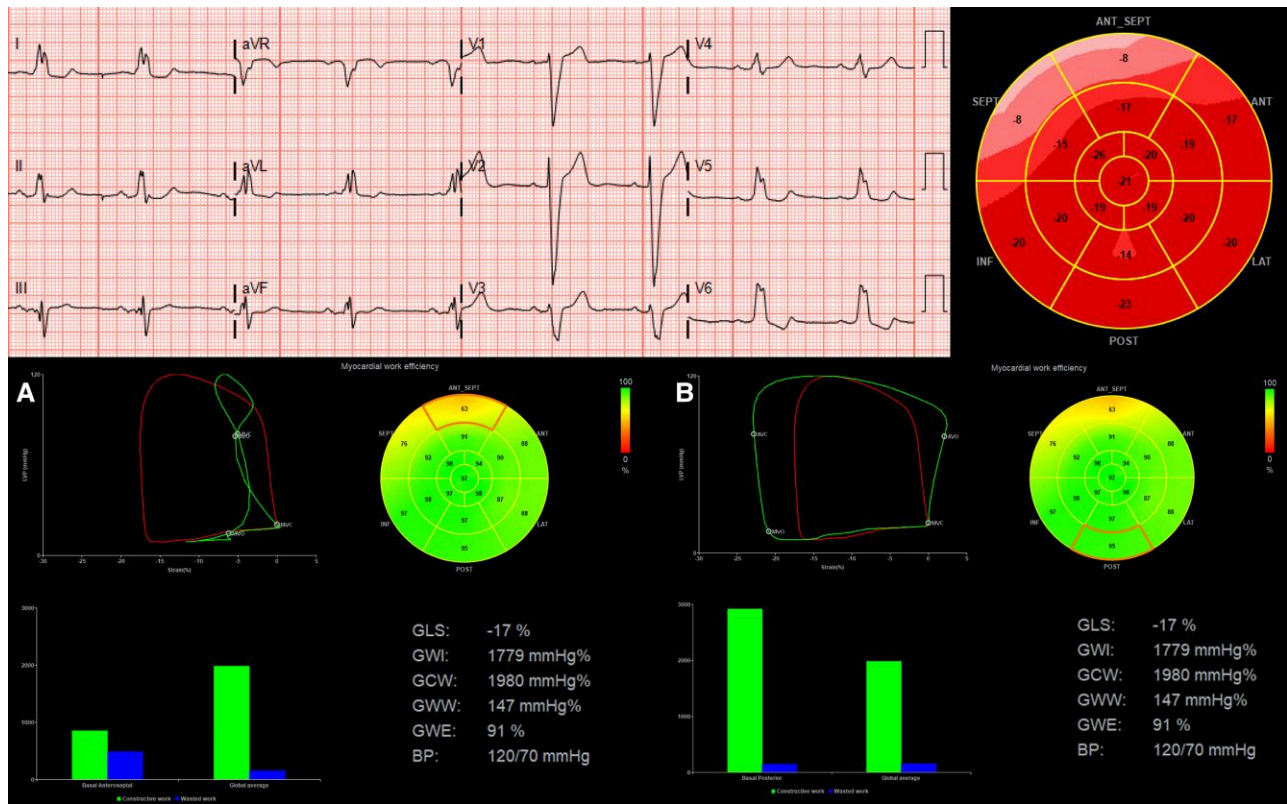


Figure 20 Myocardial work analysis in LBBB. Combining segmental LV strain measurements with estimated LV pressure allows to construct pressure-strain loops. The area of these loops reflects the performed segmental work per volume unit. Green, segmental loops of the highlighted segment; red, global loop. (A) In the basal segment of the anteroseptal wall of this patient with LBBB, a 'figure of eight' formation of the pressure-strain loop is found (green loop, corresponding with the segment highlighted in red on the bull's eye). This aspect reflects negative work, which can be interpreted as 'wasted' work compared with the constructive work performed by other parts of the ventricle. (B) The pressure-strain loop of the basal segment of the inferolateral wall (green loop corresponding with the segment highlighted in red on the bull's eye) is bigger than the average (red loop), as it has to compensate for the early activated walls.

Left atrial function

Although most of the studies investigating the role of imaging in CRT response prediction focussed on LV function, a recent study has demonstrated that baseline left atrial reservoir function, assessed with echocardiographic strain imaging, is independently associated with volumetric CRT response.¹⁵⁷ Furthermore, imaging studies have shown that left atrial reverse remodelling is independently predictive of long-term survival after CRT implantation.^{186,187}

RV function

RV function is an independent prognostic marker in CRT recipients^{188,189} and should be routinely assessed before and after device implantation. Although simple echocardiographic parameters, such as tricuspid annular plane systolic excursion, were predictive of all-cause mortality in patients undergoing CRT,¹⁹⁰ it appears that RV free wall strain provides incremental prognostic value over conventional RV function parameters in CRT recipients.^{159,191} However, it should be noted that improvement in RV function may occur in parallel with the improvement in LV function after CRT, identifying patients with the best prognosis.¹⁹²

Coronary venous anatomy assessment

The coronary venogram is a key step for CRT implantation and selecting the optimal site for LV lead placement. This is performed during

fluoroscopy at the time of CRT implantation. The placement of a lead dedicated to LV stimulation occurs most commonly via the coronary veins, targeting the LV free wall. It is thus mandatory to have precise knowledge of the coronary venous anatomy to guide lead placement and to troubleshoot potential barriers in achieving a stable lead position. The coronary sinus drains the blood collected by the network of coronary veins into the right atrium (Figure 21). The length and size of the coronary sinus is highly variable, depending on the preferential development of certain coronary veins with respect to others during the embryonic phase. Moreover, LV or biventricular dilatation and haemodynamic overload due to the underlying cardiac disease may also change the size and length of the coronary veins, displacing the AV plane and further influencing the unique anatomic pattern of the coronary venous circulation in each patient. Thus, when planning LV lead placement, it is more clinically useful to consider the vein to be targeted based on the region of the LV where the LV lead should be located, rather than any anatomic classification based on the take-off point of the vein at the CS junction (Figure 21). Based on the electromechanical delay imposed by LBBB, the mid-basal lateral, anterolateral, or posterolateral veins are the preferential lead locations.¹⁹³ The anatomical representation of these regions is obtained by recording a coronary venogram in right anterior oblique (RAO) 20–30° and left anterior oblique (LAO) 40–60°. The RAO view (similar to the two-chamber view on imaging) displays the LV regions and the coronary veins course in full length from base to apex of the heart, thereby enabling the visualization

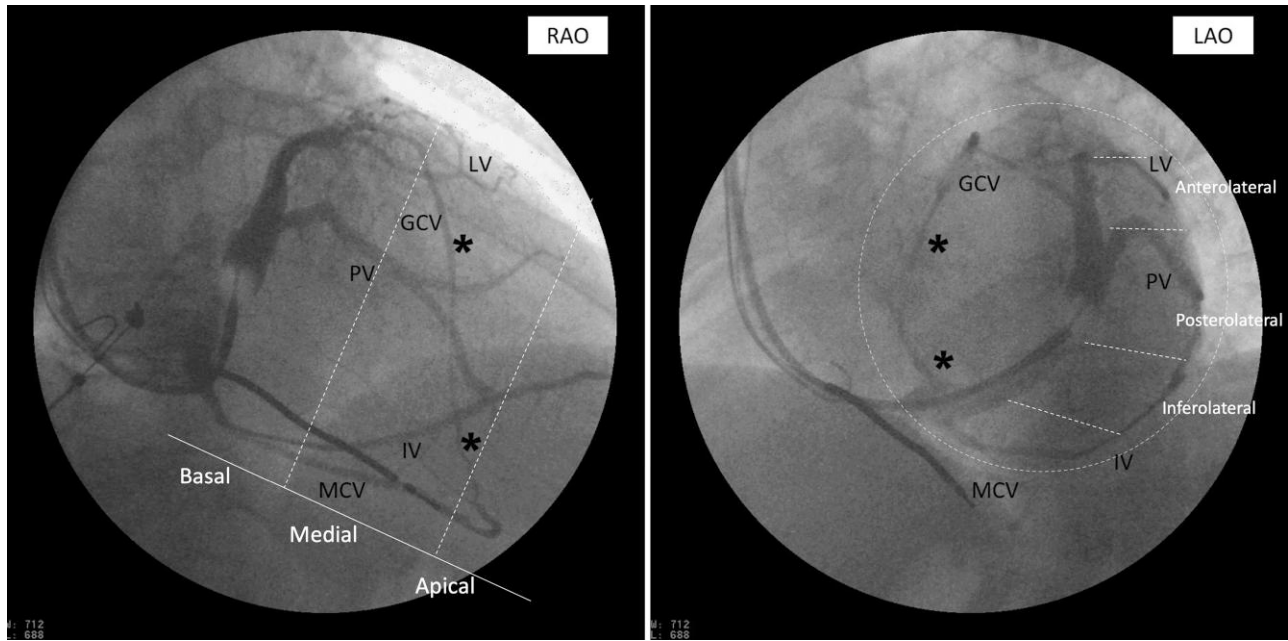


Figure 21 Coronary vein anatomy displayed in RAO and LAO views. Five tributaries of the coronary sinus with broad anastomoses of the IV and the PV, and of the MCV and GCV (also called the anterior interventricular vein). These two latter share a long anastomotic loop (*). The LV drains the lateral LV wall. The 35° RAO view enables the visualization of the LV in its basal, medial, and apical segments, whereas, in 60° LAO view, the LV lateral wall is segmented in anterolateral, posterolateral, and inferolateral regions. GCV, great cardiac vein; IV, inferior vein; LAO, left anterior oblique; LV, lateral vein; MCV, middle cardiac vein; PV, posterior coronary veins; RAO, right anterior oblique.

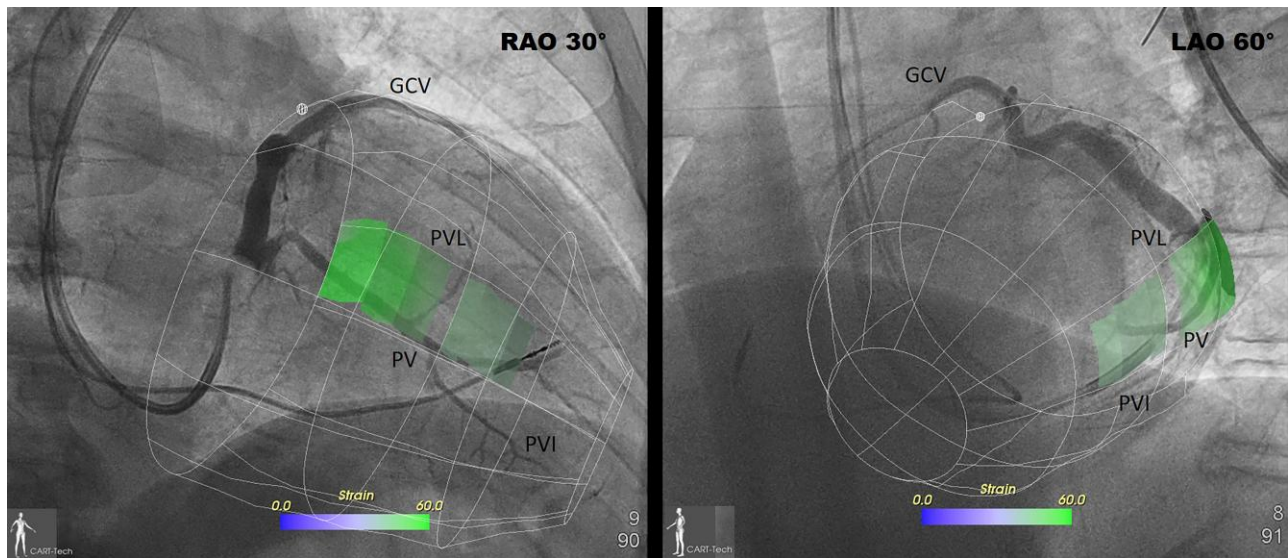


Figure 22 Cardiac resynchronization therapy intra-operative guidance for targeted LV placement: overlays of the latest mechanically activated segments on fluoroscopy during the LV lead implantation by the CARTBox system. The LV is divided into 36 segments that are shown by the wireframe. The small sphere at the basal ring of the wireframe indicates the anterior hinge point of the RV. The colours represent the latest mechanical activation of the lateral wall, which in this case is 269 ms. The lateral branch of the posterior vein (PVL) lies amidst the target area. GCV, great cardiac vein; PV, posterior vein; PVI, inferior branch of the PV.

of its basal, mid, and distal segments and the location of the junctions between the coronary veins and the coronary sinus from the middle cardiac vein inferiorly to the anterior interventricular vein and great cardiac vein superiorly (Figure 21). The LAO view (similar to the short-axis view on imaging) enables distinction of the anterior, lateral, posterior, and inferior segments of the LV (Figure 21). Separation of the LV and RV pacing leads is therefore well appreciated on this view. It is well known that coronary veins may have several connections between each other creating a venous network that spreads from the apex to the base of the heart and that ultimately drains into the coronary sinus and right atrium (Figure 21).

Anatomical variants of the thoracic venous system are not rare, with persistence of the Marshall vein or the left superior vena cava being the most common (see [Supplementary material online](#)) (Figure 3). This latter variant makes LV lead placement challenging, especially in the absence of a right superior vena cava.¹⁹⁴ Anatomic variants are more frequent in patients with congenital cardiac disease. Pre-operative cardiac imaging in these congenital heart disease patients with echocardiography, CMR, and CT scans is mandatory for proper planning of CRT procedures, to balance different opportunities during implantation. Indeed, in the event of atresia of the coronary sinus ostium (see [Supplementary material online](#)), or lack of suitable veins leading to the targeted LV location, alternative strategies such as His bundle pacing or left bundle branch area pacing may be considered before resorting to a leadless CRT implantation or to epicardial LV lead placement.¹⁹⁵ Intra-operative integration of 3D imaging with the coronary venogram in theatre can improve targeting of the most mechanically delayed and viable myocardial segments and can enhance patients' outcome (Figure 22).^{147,196–198} Of note, electrical delay to the LV lead (Q-LV interval) has also been shown to be associated with favourable outcome and may be simpler to measure than mechanical dyssynchrony parameters.¹⁹⁹

Clinical advice

Imaging is useful to assess LV mechanical dyssynchrony, myocardial scar extent and location, and RV function to obtain prognostic information in patients undergoing CRT.

Patients with CRT should be categorized as 'improved', 'unchanged', and 'worsened' on the basis of CCS rather than dichotomized as 'responders' and 'non-responders' by LV reverse remodelling or any other standalone imaging marker.

Intra-operative and, in certain cases, pre-operative imaging of the coronary venous anatomy is advisable for targeted LV lead placement.



Conclusions

In patients undergoing CIED implantation, imaging is pivotal to assess cardiac function and to potentially detect disorders causing conduction abnormalities or malignant arrhythmias. Imaging can also provide crucial information for deciding the most appropriate type of CIED and avoid problems with challenging lead placements. Randomized controlled trials are eagerly awaited to inform whether novel imaging parameters could further improve risk stratification for primary prevention of ICD implantation and refine criteria for CRT patient selection.

Supplementary data

Supplementary data are available at *European Heart Journal - Cardiovascular Imaging* online.

Funding

None declared.

Conflict of interest: I.S.: Speaker fees and software support from GE Healthcare; J.-U.V.: Speaker fees from and collaboration with GE Healthcare and Philips Ultrasound; D.M.: Collaboration with GE Healthcare; L.E.S.: Collaboration with GE Healthcare; N.A.M.: Speaker fees from GE Healthcare and Abbott Vascular and member of Medical Advisory Board of Philips Ultrasound; O.A.S. is the co-inventor of the 'Method for myocardial segment work analysis' and has filed patent on 'Estimation of blood pressure in the heart' and has one speaker fee from GE Healthcare; and E.D.: Collaboration with GE Healthcare and Abbott vascular; and H.B., K.H.H., J.L., M.B., J.-N.D., E.B., and M.R.D.: None declared.

Data availability

No new data were generated or analysed in support of this research.

References

- Raatikainen MJP, Arnar DO, Merkely B, Nielsen JC, Hindricks G, Heidbuchel H *et al.* A decade of information on the use of cardiac implantable electronic devices and interventional electrophysiological procedures in the European Society of Cardiology countries: 2017 report from the European Heart Rhythm Association. *Europace* 2017;**19**(suppl_2):iii1–ii90.
- Glikson M, Nielsen JC, Kronborg MB, Michowitz Y, Auricchio A, Barbash IM *et al.* ESC Scientific Document Group. 2021 ESC guidelines on cardiac pacing and cardiac resynchronization therapy. *Europace* 2022;**24**:71–164.
- Zeppenfeld K, Tfelt-Hansen J, de Riva M, Winkel BG, Behr ER, Blom NA *et al.* ESC Scientific Document Group. 2022 ESC guidelines for the management of patients with ventricular arrhythmias and the prevention of sudden cardiac death. *Eur Heart J* 2022;**43**:3997–4126.
- Lang RM, Badano LP, Mor-Avi V, Afilalo J, Armstrong A, Ernande L *et al.* Recommendations for cardiac chamber quantification by echocardiography in adults: an update from the American Society of Echocardiography and the European Association of Cardiovascular Imaging. *Eur Heart J Cardiovasc Imaging* 2015;**16**:233–70.
- Malm S, Frigstad S, Sagberg E, Larsson H, Skjaerpe T. Accurate and reproducible measurement of left ventricular volume and ejection fraction by contrast echocardiography: a comparison with magnetic resonance imaging. *J Am Coll Cardiol* 2004;**44**:1030–5.
- Ünlü S, Duchenne J, Mirea O, Pagourelis ED, Bézy S, Cvijic M *et al.* Impact of apical foreshortening on deformation measurements: a report from the EACVI-ASE strain standardization task force. *Eur Heart J Cardiovasc Imaging* 2020;**21**:337–43.
- Muraru D, Cecchetto A, Cucchini U, Zhou X, Lang RM, Romeo G *et al.* Intervendor consistency and accuracy of left ventricular volume measurements using three-dimensional echocardiography. *J Am Soc Echocardiogr* 2018;**31**:158–168.e1.
- Rodríguez-Zanella H, Muraru D, Secco E, Boccalini F, Azzolina D, Aruta P *et al.* Added value of 3- versus 2-dimensional echocardiography left ventricular ejection fraction to predict arrhythmic risk in patients with left ventricular dysfunction. *JACC Cardiovasc Imaging* 2019;**12**:1917–26.
- Hernández-Madrid A, Paul T, Abrams D, Aziz PF, Blom NA, Chen J *et al.* Arrhythmias in congenital heart disease: a position paper of the European Heart Rhythm Association (EHRA), Association for European Paediatric and Congenital Cardiology (AEPC), and the European Society of Cardiology (ESC) working group on grown-up congenital heart disease, endorsed by HRS, PACES, APHRS, and SOLAECE. *Europace* 2018;**20**:1719–53.
- Albouaini K, Rao A, Ramsdale D. Pacing in patients with congenital heart disease: part 1. *Br J Cardiol* 2013;**20**:117–20.
- Albouaini K, Rao A, Ramsdale D. Pacing in patients with congenital heart disease: part 2. *Br J Cardiol* 2013;**20**:151–3.
- Burri H, Starck C, Auricchio A, Biffi M, Burri M, D'Avila A *et al.* EHRA expert consensus statement and practical guide on optimal implantation technique for conventional pacemakers and implantable cardioverter-defibrillators: endorsed by the Heart Rhythm Society (HRS), the Asia Pacific Heart Rhythm Society (APHRS), and the Latin-American Heart Rhythm Society (LAHRS). *Europace* 2021;**23**:983–1008.
- DeSimone CV, Friedman PA, Noheria A, Patel NA, DeSimone DC, Bdeir S *et al.* Stroke or transient ischemic attack in patients with transvenous pacemaker or defibrillator

- and echocardiographically detected patent foramen ovale. *Circulation* 2013;**128**:1433–41.
14. Lee JZ, Agasthi P, Pasha AK, Tarin C, Tseng AS, Diehl NN et al. Stroke in patients with cardiovascular implantable electronic device infection undergoing transvenous lead removal. *Heart Rhythm* 2018;**15**:1593–600.
 15. Wang J MD, Chen H MD, Su Y MD, Ge J. Pacing lead is more easily located at RVOT septum in patients with severe tricuspid regurgitation. *Acta Cardiol* 2016;**71**:730–6.
 16. Moral S, Ballesteros E, Huguet M, Panaro A, Palet J, Evangelista A. Differential diagnosis and clinical implications of remnants of the right valve of the sinus venosus. *J Am Soc Echocardiogr* 2016;**29**:183–94.
 17. Dissmann R, Schröder J, Völler H, Behrens S. Entrapment of pacemaker lead by a large net-like Eustachian valve within the right atrium. *Clin Res Cardiol* 2006;**95**:241–3.
 18. Dissmann R, Wolthoff U, Zabel M. Double left ventricular pacing following accidental malpositioning of the right ventricular electrode during implantation of a cardiac resynchronization therapy device. *J Cardiothorac Surg* 2013;**8**:162.
 19. Rudbeck-Resdal J, Christiansen MK, Johansen JB, Nielsen JC, Bundgaard H, Jensen HK. Aetiologies and temporal trends of atrioventricular block in young patients: a 20-year nationwide study. *Europace* 2019;**21**:1710–6.
 20. Dideriksen JR, Christiansen MK, Johansen JB, Nielsen JC, Bundgaard H, Jensen HK. Long-term outcomes in young patients with atrioventricular block of unknown aetiology. *Eur Heart J* 2021;**42**:2060–8.
 21. Arbelo E, Protonotarios A, Gimeno JR, Arbustini E, Barriales-Villa R, Basso C, ESC Scientific Document Group et al. 2023 ESC guidelines for the management of cardiomyopathies. *Eur Heart J* 2023;**44**:3503–626.
 22. Donal E, Delgado V, Bucciarelli-Ducci C, Galli E, Haugaa KH, Charron P et al. 2016–18 EACVI Scientific Documents Committee. Multimodality imaging in the diagnosis, risk stratification, and management of patients with dilated cardiomyopathies: an expert consensus document from the European Association of Cardiovascular Imaging. *Eur Heart J Cardiovasc Imaging* 2019;**20**:1075–93.
 23. Habib G, Bucciarelli-Ducci C, Caforio ALP, Cardim N, Charron P, Cosyns B et al. Indian Academy of Echocardiography. Multimodality imaging in restrictive cardiomyopathies: an EACVI expert consensus document in collaboration with the “working group on myocardial and pericardial diseases” of the European Society of Cardiology endorsed by the Indian Academy of Echocardiography. *Eur Heart J Cardiovasc Imaging* 2017;**18**:1090–121.
 24. Auffret V, Lohr A, Leurent G, Martins RP, Filippi E, Coudert I et al. High-degree atrioventricular block complicating ST segment elevation myocardial infarction in the contemporary era. *Heart* 2016;**102**:40–9.
 25. Anguera I, Miro JM, Evangelista A, Cabell CH, San Roman JA, Vilacosta I et al. Periannular complications in infective endocarditis involving native aortic valves. *Am J Cardiol* 2006;**98**:1254–60.
 26. Delgado V, Ajmone Marsan N, de Waha S, Bonaros N, Brida M, Burri H et al. ESC Scientific document group. 2023 ESC guidelines for the management of endocarditis. *Eur Heart J* 2023;**44**:3948–42.
 27. Dhingra RC, Amat-y-Leon F, Pietras RJ, Wyndham C, Deedwania PC, Wu D et al. Sites of conduction disease in aortic stenosis: significance of valve gradient and calcification. *Ann Intern Med* 1977;**87**:275–80.
 28. Thompson R, Mitchell A, Ahmed M, Towers M, Yacoub M. Conduction defects in aortic valve disease. *Am Heart J* 1979;**98**:3–10.
 29. Hwang YM, Kim J, Lee JH, Kim M, Hwang J, Kim JB et al. Conduction disturbance after isolated surgical aortic valve replacement in degenerative aortic stenosis. *J Thorac Cardiovasc Surg* 2017;**154**:1556–1565.e1.
 30. Auffret V, Puri R, Urena M, Chamandi C, Rodriguez-Gabella T, Philippon F et al. Conduction disturbances after transcatheter aortic valve replacement: current Status and future perspectives. *Circulation* 2017;**136**:1049–69.
 31. Fovino L N, Cipriani A, Fabris T, Massussi M, Scotti A, Lorenzoni G et al. Anatomical predictors of pacemaker dependency after transcatheter aortic valve replacement. *Circ Arrhythm Electrophysiol* 2021;**14**:e009028.
 32. Maier O, Piayda K, Afzal S, Polzin A, Westenfeld R, Jung C et al. Computed tomography derived predictors of permanent pacemaker implantation after transcatheter aortic valve replacement: a meta-analysis. *Catheter Cardiovasc Interv* 2021;**98**:E897–E907.
 33. Sharma E, McCauley B, Ghosalkar DS, Atalay M, Collins S, Parulker A et al. Aortic valve calcification as a predictor of post-transcatheter aortic valve replacement pacemaker dependence. *Cardiol Res* 2020;**11**:155–67.
 34. Maeno Y, Abramowitz Y, Kawamori H, Kazuno Y, Kubo S, Takahashi N et al. A highly predictive risk model for pacemaker implantation after TAVR. *JACC Cardiovasc Imaging* 2017;**10**:1139–47.
 35. Ogunbayo GO, Elayi SC, Ha LD, Olorunfemi O, Elbadawi A, Saheed D et al. Outcomes of heart block in myocarditis: a review of 31,760 patients. *Heart Lung Circ* 2019;**28**:272–6.
 36. Kandolin R, Lehtonen J, Kupari M. Cardiac sarcoidosis and giant cell myocarditis as causes of atrioventricular block in young and middle-aged adults. *Circ Arrhythm Electrophysiol* 2011;**4**:303–9.
 37. Cooper LT Jr, Blauwet LA. When should high-grade heart block trigger a search for a treatable cardiomyopathy? *Circ Arrhythm Electrophysiol* 2011;**4**:260–1.
 38. Slart RHJA, Glaudemans AWJM, Lancellotti P, Hyafil F, Blankstein R, Schwartz RG et al. A joint procedural position statement on imaging in cardiac sarcoidosis: from the cardiovascular and inflammation & infection committees of the European Association of Nuclear Medicine, the European Association of Cardiovascular Imaging, and the American Society of Nuclear Cardiology. *Eur Heart J Cardiovasc Imaging* 2017;**18**:1073–89.
 39. Ferreira VM, Schulz-Menger J, Holmvang G, Kramer CM, Carbone I, Sechtem U et al. Cardiovascular magnetic resonance in nonischemic myocardial inflammation: expert recommendations. *J Am Coll Cardiol* 2018;**72**:3158–76.
 40. Donnellan E, Wazni OM, Saliba WI, Hanna M, Kanj M, Patel DR et al. Prevalence, incidence, and impact on mortality of conduction system disease in transthyretin cardiac amyloidosis. *Am J Cardiol* 2020;**128**:140–6.
 41. Garcia-Pavia P, Rapezzi C, Adler Y, Arad M, Basso C, Brucato A et al. Diagnosis and treatment of cardiac amyloidosis: a position statement of the ESC working group on myocardial and pericardial diseases. *Eur Heart J* 2021;**42**:1554–68.
 42. Cardim N, Brito D, Rocha Lopes L, Freitas A, Araújo C, Belo A et al. Participating Centres. The Portuguese registry of hypertrophic cardiomyopathy: overall results. *Rev Port Cardiol (Engl Ed)* 2018;**37**:1–10.
 43. Daubert C, Gadler F, Mabo P, Linde C. Pacing for hypertrophic obstructive cardiomyopathy: an update and future directions. *Europace* 2018;**20**:908–20.
 44. Linhart A, Kampmann C, Zamorano JL, Sunder-Plassmann G, Beck M, Mehta A et al. Cardiac manifestations of anderson-fabry disease: results from the international fabry outcome survey. *Eur Heart J* 2007;**28**:1228–35.
 45. Rapezzi C, Aimo A, Barison A, Emdin M, Porcari A, Linhart A et al. Restrictive cardiomyopathy: definition and diagnosis. *Eur Heart J* 2022;**43**:4679–93.
 46. Menghoum N, Vos JL, Pouleur AC, Nijveldt R, Gerber BL. How to evaluate cardiomyopathies by cardiovascular magnetic resonance parametric mapping and late gadolinium enhancement. *Eur Heart J Cardiovasc Imaging* 2022;**23**:587–9.
 47. Udani K, Chris-Olajia A, Ohadugha C, Malik A, Sansbury J, Paari D. Cardiovascular manifestations in hospitalized patients with hemochromatosis in the United States. *Int J Cardiol* 2021;**342**:117–24.
 48. Nunes MCP, Badano LP, Marin-Neto JA, Edvardsen T, Fernández-Golfín C, Bucciarelli-Ducci C et al. Multimodality imaging evaluation of chagas disease: an expert consensus of Brazilian Cardiovascular Imaging Department (DIC) and the European Association of Cardiovascular Imaging (EACVI). *Eur Heart J Cardiovasc Imaging* 2018;**19**:459–460.
 49. Jayaprakash S. Clinical presentations, diagnosis, and management of arrhythmias associated with cardiac tumors. *J Arrhythm* 2018;**34**:384–93.
 50. Tyebally S, Chen D, Bhattacharyya S, Mughrabi A, Hussain Z, Manisty C et al. Cardiac tumors: JACC CardioOncology state-of-the-art review. *JACC CardioOncol* 2020;**2**:293–311.
 51. Ferri LA, Farina A, Lenatti L, Ruffa F, Tiberti G, Piatti L et al. Emergent transvenous cardiac pacing using ultrasound guidance: a prospective study versus the standard fluoroscopy-guided procedure. *Eur Heart J Acute Cardiovasc Care* 2016;**5**:125–9.
 52. Bardy GH, Lee KL, Mark DB, Poole JE, Packer DL, Boineau R et al. Amiodarone or an implantable cardioverter-defibrillator for congestive heart failure. *N Engl J Med* 2005;**352**:225–37.
 53. Køber L, Thune JJ, Nielsen JC, Haarbøj J, Videbæk L, Korup E et al. Defibrillator implantation in patients with nonischemic systolic heart failure. *N Engl J Med* 2016;**375**:1221–30.
 54. Watanabe E, Abbasi SA, Heydari B, Coelho-Filho OR, Shah R, Neilan TG et al. Infarct tissue heterogeneity by contrast-enhanced magnetic resonance imaging is a novel predictor of mortality in patients with chronic coronary artery disease and left ventricular dysfunction. *Circ Cardiovasc Imaging* 2014;**7**:887–94.
 55. Roes SD, Borleffs CJ, van der Geest RJ, Westenberg JJ, Marsan NA, Kaandorp TA et al. Infarct tissue heterogeneity assessed with contrast-enhanced MRI predicts spontaneous ventricular arrhythmia in patients with ischemic cardiomyopathy and implantable cardioverter-defibrillator. *Circ Cardiovasc Imaging* 2009;**2**:183–90.
 56. Disertori M, Rigoni M, Pace N, Casolo G, Masè M, Gonzini L et al. Myocardial fibrosis assessment by LGE is a powerful predictor of ventricular tachyarrhythmias in ischemic and nonischemic LV dysfunction: a meta-analysis. *JACC Cardiovasc Imaging* 2016;**9**:1046–55.
 57. Soslow JH, Damon SM, Crum K, Lawson MA, Slaughter JC, Xu M et al. Increased myocardial native T1 and extracellular volume in patients with duchenne muscular dystrophy. *J Cardiovasc Magn Reson* 2016;**18**:5.
 58. Selvanayagam JB, Hartshorne T, Billot L, Grover S, Hillis GS, Jung W et al. Cardiovascular magnetic resonance-GUIDEd management of mild to moderate left ventricular systolic dysfunction (CMR GUIDE): study protocol for a randomized controlled trial. *Ann Noninvasive Electrocardiol* 2017;**22**:e12420.
 59. Guerra F, Malagoli A, Contadini D, Baiocco E, Menditto A, Bonelli P et al. Global longitudinal strain as a predictor of first and subsequent arrhythmic events in remotely monitored ICD patients with structural heart disease. *JACC Cardiovasc Imaging* 2020;**13**(1 Pt 1):1–9.

60. Haugaa KH, Amlie JP, Berge KE, Leren TP, Smiseth OA, Edvardsen T. Transmural differences in myocardial contraction in long-QT syndrome: mechanical consequences of ion channel dysfunction. *Circulation* 2010;**122**:1355–63.
61. Haugaa KH, Smedsrud MK, Steen T, Kongsgaard E, Loennechen JP, Skjaerpe T *et al*. Mechanical dispersion assessed by myocardial strain in patients after myocardial infarction for risk prediction of ventricular arrhythmia. *JACC Cardiovasc Imaging* 2010;**3**:247–56.
62. Muser D, Tioni C, Shah R, Selvanayagam JB, Nucifora G. Prevalence, correlates, and prognostic relevance of myocardial mechanical dispersion as assessed by feature-tracking cardiac magnetic resonance after a first ST-segment elevation myocardial infarction. *Am J Cardiol* 2017;**120**:527–33.
63. Haugaa KH, Hasselberg NE, Edvardsen T. Mechanical dispersion by strain echocardiography: a predictor of ventricular arrhythmias in subjects with lamin A/C mutations. *JACC Cardiovasc Imaging* 2015;**8**:104–6.
64. Gimelli A, Liga R, Agostini D, Bengel FM, Ernst S, Hyafil F *et al*. The role of myocardial innervation imaging in different clinical scenarios: an expert document of the European association of cardiovascular imaging and cardiovascular committee of the European association of nuclear medicine. *Eur Heart J Cardiovasc Imaging* 2021;**22**:480–90.
65. Al Badarin FJ, Wimmer AP, Kennedy KF, Jacobson AF, Bateman TM. The utility of ADMIRE-HF risk score in predicting serious arrhythmic events in heart failure patients: incremental prognostic benefit of cardiac 123I-mIBG scintigraphy. *J Nucl Cardiol* 2014;**21**:756–62; quiz 753–55, 763–5.
66. Fallavollita JA, Heavey BM, Luisi AJ Jr, Michalek SM, Baldwa S, Mashtare TL Jr *et al*. Regional myocardial sympathetic denervation predicts the risk of sudden cardiac arrest in ischemic cardiomyopathy. *J Am Coll Cardiol* 2014;**63**:141–9.
67. Piccini JP, Starr AZ, Horton JR, Shaw LK, Lee KL, Al-Khatib SM *et al*. Single-photon emission computed tomography myocardial perfusion imaging and the risk of sudden cardiac death in patients with coronary disease and left ventricular ejection fraction > 35%. *J Am Coll Cardiol* 2010;**56**:206–14.
68. Blankstein R, Osborne M, Naya M, Waller A, Kim CK, Murthy VL *et al*. Cardiac positron emission tomography enhances prognostic assessments of patients with suspected cardiac sarcoidosis. *J Am Coll Cardiol* 2014;**63**:329–36.
69. Andreini D, Conte E, Mushtaq A, Melotti E, Gigante C, Mancini ME *et al*. Comprehensive evaluation of left ventricle dysfunction by a new computed tomography scanner: the E-PLURIBUS study. *JACC Cardiovasc Imaging* 2023;**16**:175–88.
70. Conte E, Mushtaq S, Carbuicchio C, Piperno G, Catto V, Mancini ME *et al*. State of the art paper: cardiovascular CT for planning ventricular tachycardia ablation procedures. *J Cardiovasc Comput Tomogr* 2021;**15**:394–402.
71. Conte E, Carbuicchio C, Catto V, Kochi AN, Mushtaq S, De Luliis PG *et al*. Live integration of comprehensive cardiac CT with electroanatomical mapping in patients with refractory ventricular tachycardia. *J Cardiovasc Comput Tomogr* 2022;**16**:262–5.
72. Carbuicchio C, Andreini D, Piperno G, Catto V, Conte E, Cattani F *et al*. Stereotactic radioablation for the treatment of ventricular tachycardia: preliminary data and insights from the STRA-MI-VT phase Ib/II study. *J Interv Card Electrophysiol* 2021;**62**:427–39.
73. Kubala M, de Chillou C, Bohot V, Lancellotti P, Enriquez-Sarano M, Tribouilloy C. Arrhythmias in patients with valvular heart disease: gaps in knowledge and the way forward. *Front Cardiovasc Med* 2022;**9**:792559.
74. Everett RJ, Tastet L, Clavel MA, Chin CWL, Capoulade R, Vassiliou VS *et al*. Progression of hypertrophy and myocardial fibrosis in aortic stenosis: a multicenter cardiac magnetic resonance study. *Circ Cardiovasc Imaging* 2018;**11**:e007451.
75. Levine RA, Triulzi MO, Harrigan P, Weyman AE. The relationship of mitral annular shape to the diagnosis of mitral valve prolapse. *Circulation* 1987;**75**:756–67.
76. Hutchins GM, Moore DKS. The association of floppy mitral valve with disjunction of the mitral annulus fibrosus. *N Engl J Med* 1986;**314**:535–40.
77. Sabbag A, Essayagh B, Barrera JDR, Basso C, Berni A, Cosyns B *et al*. EHRA expert consensus statement on arrhythmic mitral valve prolapse and mitral annular disjunction complex in collaboration with the ESC council on valvular heart disease and the European Association of Cardiovascular Imaging endorsed by the Heart Rhythm Society, by the Asia Pacific Heart Rhythm Society, and by the Latin American Heart Rhythm Society. *Europace* 2022;**24**:1981–2003.
78. Zugwiz D, Fung K, Aung N, Rauseo E, McCracken C, Cooper J *et al*. Mitral annular disjunction assessed using CMR imaging: insights from the UK biobank population study. *JACC Cardiovasc Imaging* 2022;**15**:1856–66.
79. Chivulescu M, Aabel WE, Gjertsen E, Hopp E, Scheirlynck E, Cosyns B *et al*. Electrical markers and arrhythmic risk associated with myocardial fibrosis in mitral valve prolapse. *Europace* 2022;**24**:1156–63.
80. Aquaro GD, Perfetti M, Camastra G, Monti L, Dellegrottaglie S, Moro C *et al*. Cardiac MR with late gadolinium enhancement in acute myocarditis with preserved systolic function: ITAMY study. *J Am Coll Cardiol* 2017;**70**:1977–87.
81. Al-Khatib SM, Stevenson WG, Ackerman MJ, Bryant WJ, Callans DJ, Curtis AB *et al*. 2017 AHA/ACC/HRS guideline for management of patients with ventricular arrhythmias and the prevention of sudden cardiac death: a report of the American College of Cardiology/American Heart Association task force on clinical practice guidelines and the Heart Rhythm Society. *J Am Coll Cardiol* 2018;**72**:e91–e220.
82. Coleman GC, Shaw PW, Balfour PC Jr, Gonzalez JA, Kramer CM, Patel AR *et al*. Prognostic value of myocardial scarring on CMR in patients with cardiac sarcoidosis. *JACC Cardiovasc Imaging* 2017;**10**:411–20.
83. Kazmirczak F, Chen KA, Adabag S, von Wald L, Roukoz H, Benditt DG *et al*. Assessment of the 2017 AHA/ACC/HRS guideline recommendations for implantable cardioverter-defibrillator implantation in cardiac sarcoidosis. *Circ Arrhythm Electrophysiol* 2019;**12**:e007488.
84. Ekström K, Lehtonen J, Hänninen H, Kandolin R, Kivistö S, Kupari M. Magnetic resonance imaging as a predictor of survival free of life-threatening arrhythmias and transplantation in cardiac sarcoidosis. *J Am Heart Assoc* 2016;**5**:e003040.
85. Ise T, Hasegawa T, Morita Y, Yamada N, Funada A, Takahama H *et al*. Extensive late gadolinium enhancement on cardiovascular magnetic resonance predicts adverse outcomes and lack of improvement in LV function after steroid therapy in cardiac sarcoidosis. *Heart* 2014;**100**:1165–72.
86. Crawford T, Mueller G, Sarsam S, Prasitdumrong H, Chaiyen N, Gu X *et al*. Magnetic resonance imaging for identifying patients with cardiac sarcoidosis and preserved or mildly reduced left ventricular function at risk of ventricular arrhythmias. *Circ Arrhythm Electrophysiol* 2014;**7**:1109–15.
87. Guta AC, Badano LP, Ochoa-Jimenez RC, Genovese D, Previtero M, Civera S *et al*. Three-dimensional echocardiography to assess left ventricular geometry and function. *Expert Rev Cardiovasc Ther* 2019;**17**:801–15.
88. Elliott PM, Anastakis A, Borger MA, Borggrefe M, Cecchi F, Charron P *et al*. 2014 ESC guidelines on diagnosis and management of hypertrophic cardiomyopathy: the task force for the diagnosis and management of hypertrophic cardiomyopathy of the European Society of Cardiology (ESC). *Eur Heart J* 2014;**35**:2733–79.
89. Monserrat L, Elliott PM, Gimeno JR, Sharma S, Penas-Lado M, McKenna WJ. Non-sustained ventricular tachycardia in hypertrophic cardiomyopathy: an independent marker of sudden death risk in young patients. *J Am Coll Cardiol* 2003;**42**:873–9.
90. Chan RH, Maron BJ, Olivetto I, Pencina MJ, Assenza GE, Haas T *et al*. Prognostic value of quantitative contrast-enhanced cardiovascular magnetic resonance for the evaluation of sudden death risk in patients with hypertrophic cardiomyopathy. *Circulation* 2014;**130**:484–95.
91. Mentias A, Raesi-Giglou P, Smedira NG, Feng K, Sato K, Wazni O *et al*. Late gadolinium enhancement in patients with hypertrophic cardiomyopathy and preserved systolic function. *J Am Coll Cardiol* 2018;**72**:857–70.
92. Haugaa KH, Bundgaard H, Edvardsen T, Eschen O, Gilljam T, Hansen J *et al*. Management of patients with arrhythmogenic right ventricular cardiomyopathy in the Nordic countries. *Scand Cardiovasc J* 2015;**49**:299–307.
93. Leren IS, Saberniak J, Haland TF, Edvardsen T, Haugaa KH. Combination of ECG and echocardiography for identification of arrhythmic events in early ARVC. *JACC Cardiovasc Imaging* 2017;**10**:503–13.
94. Lie ØH, Rootwelt-Norberg C, Dejgaard LA, Leren IS, Stokke MK, Edvardsen T *et al*. Prediction of life-threatening ventricular arrhythmia in patients with arrhythmogenic cardiomyopathy: a primary prevention cohort study. *JACC Cardiovasc Imaging* 2018;**11**:1377–86.
95. Kirkels FP, Lie ØH, Cramer MJ, Chivulescu M, Rootwelt-Norberg C, Asselbergs FW *et al*. Right ventricular functional abnormalities in arrhythmogenic cardiomyopathy: association with life-threatening ventricular arrhythmias. *JACC Cardiovasc Imaging* 2021;**14**:900–10.
96. Corrado D, Leoni L, Link MS, Della Bella P, Gaita F, Curnis A *et al*. Implantable cardioverter-defibrillator therapy for prevention of sudden death in patients with arrhythmogenic right ventricular cardiomyopathy/dysplasia. *Circulation* 2003;**108**:3084–91.
97. Cadrin-Tourigny J, Bosman LP, Nozza A, Wang W, Tadros R, Bhonsale A *et al*. A new prediction model for ventricular arrhythmias in arrhythmogenic right ventricular cardiomyopathy. *Eur Heart J* 2019;**40**:1850–8.
98. Cadrin-Tourigny J, Bosman LP, Wang W, Tadros R, Bhonsale A, Bourfiss M *et al*. Sudden cardiac death prediction in arrhythmogenic right ventricular cardiomyopathy: A multinational collaboration. *Circ Arrhythm Electrophysiol* 2021;**14**:e008509.
99. Taha K, Kirkels FP, Teske AJ, Asselbergs FW, van Tintelen JP, Doevendans PA *et al*. Echocardiographic deformation imaging for early detection of genetic cardiomyopathies: JACC review topic of the week. *J Am Coll Cardiol* 2022;**79**:594–608.
100. Christensen AH, Platonov PG, Svensson A, Jensen HK, Rootwelt-Norberg C, Dahlberg P *et al*. Complications of implantable cardioverter-defibrillator treatment in arrhythmogenic right ventricular cardiomyopathy. *Europace* 2022;**24**:306–12.
101. Mugnai G, Tomei R, Dugo C, Tomasi L, Morani G, Vassanelli C. Implantable cardioverter-defibrillators in patients with arrhythmogenic right ventricular cardiomyopathy: the course of electronic parameters, clinical features, and complications during long-term follow-up. *J Interv Card Electrophysiol* 2014;**41**:23–9.
102. Gati S, Rajani R, Carr-White GS, Chambers JB. Adult left ventricular noncompaction: reappraisal of current diagnostic imaging modalities. *JACC Cardiovasc Imaging* 2014;**7**:1266–75.
103. McDonagh TA, Metra M, Adamo M, Gardner RS, Baumhach A, Böhm M *et al*. ESC Scientific Document Group. 2021 ESC guidelines for the diagnosis and treatment of acute and chronic heart failure. *Eur Heart J* 2021;**42**:3599–726.

104. Hasselberg NE, Edvardsen T, Petri H, Berge KE, Leren TP, Bundgaard H et al. Risk prediction of ventricular arrhythmias and myocardial function in lamin A/C mutation positive subjects. *Europace* 2014;**16**:563–71.
105. Sidhu K, Castrini AI, Parikh V, Reza N, Owens A, Tremblay-Gravel M et al. The response to cardiac resynchronization therapy in LMNA cardiomyopathy. *Eur J Heart Fail* 2022;**24**:685–93.
106. Scheirlyncx E, Chivulescu M, Lie ØH, Motoc A, Koulalis J, de Asmundis C et al. Worse prognosis in Brugada syndrome patients with arrhythmogenic cardiomyopathy features. *JACC Clin Electrophysiol* 2020;**6**:1353–63.
107. Corrado D, Zorzi A, Cerrone M, Rigato I, Mongillo M, Bauce B et al. Relationship between arrhythmogenic right ventricular cardiomyopathy and Brugada syndrome: new insights from molecular biology and clinical implications. *Circ Arrhythm Electrophysiol* 2016;**9**:e003631.
108. Scheirlyncx E, Van Malderen S, Motoc A, Lie ØH, de Asmundis C, Sieira J et al. Contraction alterations in Brugada syndrome; association with life-threatening ventricular arrhythmias. *Int J Cardiol* 2020;**299**:147–52.
109. Beela AS, Ünlü S, Duchenne J, Ciarka A, Daraban AM, Kotrc M et al. Assessment of mechanical dyssynchrony can improve the prognostic value of guideline-based patient selection for cardiac resynchronization therapy. *Eur Heart J Cardiovasc Imaging* 2019;**20**:66–74.
110. Dickstein K, Vardas PE, Auricchio A, Daubert JC, Linde C, McMurray J et al. ESC Committee for Practice Guidelines (CPG). 2010 focused update of ESC guidelines on device therapy in heart failure: an update of the 2008 ESC guidelines for the diagnosis and treatment of acute and chronic heart failure and the 2007 ESC guidelines for cardiac and resynchronization therapy. Developed with the special contribution of the Heart Failure Association and the European Heart Rhythm Association. *Eur Heart J* 2010;**31**:2677–87.
111. Chung ES, Leon AR, Tavazzi L, Sun JP, Nihoyannopoulos P, Merlino J et al. Results of the Predictors of Response to CRT (PROSPECT) trial. *Circulation* 2008;**117**:2608–16.
112. Ruschitzka F, Abraham WT, Singh JP, Bax JJ, Borer JS, Brugada J et al. Cardiac-resynchronization therapy in heart failure with a narrow QRS complex. *N Engl J Med* 2013;**369**:1395–405.
113. Szulik M, Tillekaerts M, Vangeel V, Ganame J, Willems R, Lenarczyk R et al. Assessment of apical rocking: a new, integrative approach for selection of candidates for cardiac resynchronization therapy. *Eur J Echocardiogr* 2010;**11**:863–9.
114. Stankovic I, Prinz C, Ciarka A, Daraban AM, Kotrc M, Aarones M et al. Relationship of visually assessed apical rocking and septal flash to response and long-term survival following cardiac resynchronization therapy (PREDICT-CRT). *Eur Heart J Cardiovasc Imaging* 2016;**17**:262–9.
115. Aalen JM, Donal E, Larsen CK, Duchenne J, Lederlin M, Cvijic M et al. Imaging predictors of response to cardiac resynchronization therapy: left ventricular work asymmetry by echocardiography and septal viability by cardiac magnetic resonance. *Eur Heart J* 2020;**41**:3813–23.
116. Górcsan J III, Anderson CP, Tayal B, Sugahara M, Walmsley J, Starling RC et al. Systolic stretch characterizes the electromechanical substrate responsive to cardiac resynchronization therapy. *JACC Cardiovasc Imaging* 2019;**12**:1741–52.
117. Risum N, Jons C, Olsen NT, Fritz-Hansen T, Bruun NE, Hojgaard MV et al. Simple regional strain pattern analysis to predict response to cardiac resynchronization therapy: rationale, initial results, and advantages. *Am Heart J* 2012;**163**:697–704.
118. Chung ES, Gold MR, Abraham WT, Young JB, Linde C, Anderson C et al. The importance of early evaluation after cardiac resynchronization therapy to redefine response: pooled individual patient analysis from 5 prospective studies. *Heart Rhythm* 2022;**19**:595–603.
119. Stankovic I, Belmans A, Prinz C, Ciarka A, Daraban AM, Kotrc M et al. The association of volumetric response and long-term survival after cardiac resynchronization therapy. *Eur Heart J Cardiovasc Imaging* 2017;**18**:1109–17.
120. Mullens W, Verga T, Grimm RA, Starling RC, Wilkoff BL, Tang WH. Persistent hemodynamic benefits of cardiac resynchronization therapy with disease progression in advanced heart failure. *J Am Coll Cardiol* 2009;**53**:600–7.
121. Packer M. Proposal for a new clinical end point to evaluate the efficacy of drugs and devices in the treatment of chronic heart failure. *J Card Fail* 2001;**7**:176–82.
122. Cazeau S, Leclercq C, Lavergne T, Walker S, Varma C, Linde C et al. Effects of multisite biventricular pacing in patients with heart failure and intraventricular conduction delay. *N Engl J Med* 2001;**344**:873–80.
123. Jones S, Lumens J, Sohaib SMA, Finegold JA, Kanagaratnam P, Tanner M et al. Cardiac resynchronization therapy: mechanisms of action and scope for further improvement in cardiac function. *Europace* 2017;**19**:1178–86.
124. Górcsan J III, Oyenuga O, Habib PJ, Tanaka H, Adelstein EC, Hara H et al. Relationship of echocardiographic dyssynchrony to long-term survival after cardiac resynchronization therapy. *Circulation* 2010;**122**:1910–8.
125. Delgado V, Van Bommel RJ, Bertini M, Borleffs CJ, Marsan NA, Arnold CT et al. Relative merits of left ventricular dyssynchrony, left ventricular lead position, and myocardial scar to predict long-term survival of ischemic heart failure patients undergoing cardiac resynchronization therapy. *Circulation* 2011;**123**:70–8.
126. Richardson M, Freemantle N, Calvert MJ, Cleland JG, Tavazzi L. Predictors and treatment response with cardiac resynchronization therapy in patients with heart failure characterized by dyssynchrony: a pre-defined analysis from the CARE-HF trial. *Eur Heart J* 2007;**28**:1827–34.
127. Zhang Q, van Bommel RJ, Fung JW, Chan JY, Bleeker GB, Ypenburg C et al. Tissue Doppler velocity is superior to strain imaging in predicting long-term cardiovascular events after cardiac resynchronization therapy. *Heart* 2009;**95**:1085–90.
128. Lumens J, Leenders GE, Cramer MJ, De Boeck BW, Doevendans PA, Prinzen FW et al. Mechanistic evaluation of echocardiographic dyssynchrony indices: patient data combined with multiscale computer simulations. *Circ Cardiovasc Imaging* 2012;**5**:491–9.
129. Leenders GE, Lumens J, Cramer MJ, De Boeck BW, Doevendans PA, Delhaas T et al. Septal deformation patterns delineate mechanical dyssynchrony and regional differences in contractility: analysis of patient data using a computer model. *Circ Heart Fail* 2012;**5**:87–96.
130. Calle S, Kamoen V, De Buyzere M, De Pooter J, Timmermans F. A strain-based staging classification of left bundle branch block-induced cardiac remodeling. *JACC Cardiovasc Imaging* 2021;**14**:1691–702.
131. Vernoooy K, Verbeek XA, Peschar M, Crijns HJ, Arts T, Cornelussen RN et al. Left bundle branch block induces ventricular remodeling and functional septal hypoperfusion. *Eur Heart J* 2005;**26**:91–8.
132. Duchenne J, Claus P, Pagourelis ED, Mada RO, Van Puyvelde J, Vunckx K et al. Sheep can be used as animal model of regional myocardial remodeling and controllable work. *Cardiol J* 2019;**26**:375–84.
133. Voigt JU, Lindenmeier G, Exner B, Regenfus M, Werner D, Reulbach U et al. Incidence and characteristics of segmental postsystolic longitudinal shortening in normal, acutely ischemic, and scarred myocardium. *J Am Soc Echocardiogr* 2003;**16**:415–23.
134. Lumens J, Tayal B, Walmsley J, Delgado-Montero A, Huntjens PR, Schwartzman D et al. Differentiating electromechanical from non-electrical substrates of mechanical dyssynchronization to identify responders to cardiac resynchronization therapy. *Circ Cardiovasc Imaging* 2015;**8**:e003744.
135. Aalen JM, Remme EV, Larsen CK, Andersen OS, Krogh M, Duchenne J et al. Mechanism of abnormal septal motion in left bundle branch block: role of left ventricular wall interactions and myocardial scar. *JACC Cardiovasc Imaging* 2019;**12**:2402–13.
136. Badano LP, Cucchini U, Muraru D, Ai Nono O, Sarais C, Illiceto S. Use of three-dimensional speckle tracking to assess left ventricular myocardial mechanics: inter-vendor consistency and reproducibility of strain measurements. *Eur Heart J Cardiovasc Imaging* 2013;**14**:285–93.
137. Morton G, Schuster A, Jogiya R, Kutty S, Beerbaum P, Nagel E. Inter-study reproducibility of cardiovascular magnetic resonance myocardial feature tracking. *J Cardiovasc Magn Reson* 2012;**14**:43.
138. Barreiro-Pérez M, Curione D, Symons R, Claus P, Voigt JU, Bogaert J. Left ventricular global myocardial strain assessment comparing the reproducibility of four commercially available CMR-feature tracking algorithms. *Eur Radiol* 2018;**28**:5137–47.
139. Bernhard B, Grogg H, Zurkirchen J, Demirel C, Hagemeyer D, Okuno T et al. Reproducibility of 4D cardiac computed tomography feature tracking myocardial strain and comparison against speckle-tracking echocardiography in patients with severe aortic stenosis. *J Cardiovasc Comput Tomogr* 2022;**16**:309–18.
140. Boogers MM, Van Kriekinge SD, Henneken MM, Ypenburg C, Van Bommel RJ, Boersma E et al. Quantitative gated SPECT-derived phase analysis on gated myocardial perfusion SPECT detects left ventricular dyssynchrony and predicts response to cardiac resynchronization therapy. *J Nucl Med* 2009;**50**:718–25.
141. Tang H, Tang S, Zhou W. A review of image-guided approaches for cardiac resynchronization therapy. *Arrhythm Electrophysiol Rev* 2017;**6**:69–74.
142. Acosta J, Fernández-Armenta J, Borràs R, Anguera I, Bisbal F, Martí-Almor J et al. Scar characterization to predict life-threatening arrhythmic events and sudden cardiac death in patients with cardiac resynchronization therapy: the GAUDI-CRT study. *JACC Cardiovasc Imaging* 2018;**11**:561–72.
143. Bleeker GB, Kaandorp TA, Lamb HJ, Boersma E, Steendijk P, de Roos A et al. Effect of posterolateral scar tissue on clinical and echocardiographic improvement after cardiac resynchronization therapy. *Circulation* 2006;**113**:969–76.
144. Leyva F, Foley PV, Chali S, Ratib K, Smith RE, Prinzen F et al. Cardiac resynchronization therapy guided by late gadolinium-enhancement cardiovascular magnetic resonance. *J Cardiovasc Magn Reson* 2011;**13**:29.
145. Steelant B, Stankovic I, Roijackers I, Aarones M, Bogaert J, Desmet W et al. The impact of infarct location and extent on LV motion patterns: implications for dyssynchrony assessment. *JACC Cardiovasc Imaging* 2016;**9**:655–64.
146. Taylor RJ, Umar F, Panting JR, Stegemann B, Leyva F. Left ventricular lead position, mechanical activation, and myocardial scar in relation to left ventricular reverse remodeling and clinical outcomes after cardiac resynchronization therapy: a feature-tracking and contrast-enhanced cardiovascular magnetic resonance study. *Heart Rhythm* 2016;**13**:481–9.
147. Bertini M, Mele D, Malagù M, Fiorencis A, Toselli T, Casadei F et al. Cardiac resynchronization therapy guided by multimodality cardiac imaging. *Eur J Heart Fail* 2016;**18**:1375–82.

148. Saba S, Marek J, Schwartzman D, Jain S, Adelstein E, White P *et al*. Echocardiography-guided left ventricular lead placement for cardiac resynchronization therapy: results of the Speckle Tracking Assisted Resynchronization Therapy for Electrode Region trial. *Circ Heart Fail* 2013;**6**:427–34.
149. Kristensen J, Jensen HK, Fyenbo DB, Bouchelouche K, Nielsen JC. Electrically vs. imaging-guided left ventricular lead placement in cardiac resynchronization therapy: a randomized controlled trial. *Europace* 2019;**21**:1369–77.
150. Nowak B, Sinha AM, Schaefer WM, Koch KC, Kaiser HJ, Hanrath P *et al*. Cardiac resynchronization therapy homogenizes myocardial glucose metabolism and perfusion in dilated cardiomyopathy and left bundle branch block. *J Am Coll Cardiol* 2003;**41**:1523–8.
151. Masci PG, Marinelli M, Piacenti M, Lorenzoni V, Positano V, Lombardi M *et al*. Myocardial structural, perfusion, and metabolic correlates of left bundle branch block mechanical derangement in patients with dilated cardiomyopathy: a tagged cardiac magnetic resonance and positron emission tomography study. *Circ Cardiovasc Imaging* 2010;**3**:482–90.
152. Thompson K, Saab G, Birnie D, Chow BJ, Ukkonen H, Ananthasubramanian K *et al*. Is septal glucose metabolism altered in patients with left bundle branch block and ischemic cardiomyopathy? *J Nucl Med* 2006;**47**:1763–8.
153. Nelson GS, Berger RD, Fetis BJ, Talbot M, Spinelli JC, Hare JM *et al*. Left ventricular or biventricular pacing improves cardiac function at diminished energy cost in patients with dilated cardiomyopathy and left bundle-branch block. *Circulation* 2000;**102**:3053–9.
154. Deif B, Ballantyne B, Almeshadi F, Mikhail M, McIntyre WF, Manlucu J *et al*. Cardiac resynchronization is pro-arrhythmic in the absence of reverse ventricular remodeling: a systematic review and meta-analysis. *Cardiovasc Res* 2018;**114**:1435–44.
155. Ypenburg C, van Bommel RJ, Borleffs CJ, Bleeker GB, Boersma E, Schalij MJ *et al*. Long-term prognosis after cardiac resynchronization therapy is related to the extent of left ventricular reverse remodeling at midterm follow-up. *J Am Coll Cardiol* 2009;**53**:483–90.
156. Michalski B, Stankovic I, Pagourelas E, Ciarka A, Aarones M, Winter S *et al*. Relationship of mechanical dyssynchrony and LV remodeling with improvement of mitral regurgitation after CRT. *JACC Cardiovasc Imaging* 2022;**15**:212–20.
157. Galli E, Oger E, Aalen JM, Duchenne J, Larsen CK, Sade E *et al*. Left atrial strain is a predictor of left ventricular systolic and diastolic reverse remodeling in CRT candidates. *Eur Heart J Cardiovasc Imaging* 2022;**23**:1373–82.
158. Sade LE, Atar I, Özün B, Yüce D, Müderrisoğlu H. Determinants of new-onset atrial fibrillation in patients receiving CRT: mechanistic insights from speckle tracking imaging. *JACC Cardiovasc Imaging* 2016;**9**:99–111.
159. Sade LE, Özün B, Atar I, Demir Ö, Demirtaş S, Müderrisoğlu H. Right ventricular function is a determinant of long-term survival after cardiac resynchronization therapy. *J Am Soc Echocardiogr* 2013;**26**:706–13.
160. Yuyun MF, Erqou SA, Peralta AO, Hoffmeister PS, Yarmohammadi H, Echouffo Tcheguigui JB *et al*. Risk of ventricular arrhythmia in cardiac resynchronization therapy responders and super-responders: a systematic review and meta-analysis. *Europace* 2021;**23**:1262–74.
161. Fornwalt BK, Sprague WW, BeDell P, Suever JD, Gerritse B, Merlino JD *et al*. Agreement is poor among current criteria used to define response to cardiac resynchronization therapy. *Circulation* 2010;**121**:1985–91.
162. Boidol J, Sredniawa B, Kowalski O, Szulik M, Mazurek M, Sokal A *et al*. Many response criteria are poor predictors of outcomes after cardiac resynchronization therapy: validation using data from the randomized trial. *Europace* 2013;**15**:835–44.
163. Birnie DH, Tang AS. The problem of non-response to cardiac resynchronization therapy. *Curr Opin Cardiol* 2006;**21**:20–6.
164. Lafitte S, Reant P, Zaroui A, Donal E, Mignot A, Bougterd H *et al*. Validation of an echocardiographic multiparametric strategy to increase responders patients after cardiac resynchronization: a multicentre study. *Eur Heart J* 2009;**30**:2880–7.
165. Yu CM, Bleeker GB, Fung JW, Schalij MJ, Zhang Q, van der Wall EE *et al*. Left ventricular reverse remodeling but not clinical improvement predicts long-term survival after cardiac resynchronization therapy. *Circulation* 2005;**112**:1580–6.
166. Linde C, Gold MR, Abraham WT, St John SM, Ghio S, Cerkenjic J *et al*. Long-term impact of cardiac resynchronization therapy in mild heart failure: 5-year results from the REsynchronization reVErse remodeling in systolic left vEntricular dysfunction (REVERSE) study. *Eur Heart J* 2013;**34**:2592–99.
167. Varma N, Boehmer J, Bhargava K, Yoo D, Leonelli F, Costanzo M *et al*. Evaluation, Management, and Outcomes of Patients Poorly Responsive to Cardiac Resynchronization Device Therapy. *J Am Coll Cardiol* 2019;**74**(21):2588–603.
168. Gold MR, Rickard J, Daubert JC, Zimmerman P, Linde C. Redefining the classifications of response to cardiac resynchronization therapy: results from the REVERSE study. *JACC Clin Electrophysiol* 2021;**7**:871–80.
169. Martens P, Nijst P, Verbrugge FH, Dupont M, Tang WHW, Mullens W. Profound differences in prognostic impact of left ventricular reverse remodeling after cardiac resynchronization therapy relate to heart failure etiology. *Heart Rhythm* 2018;**15**:130–6.
170. Steffel J, Ruschitzka F. Superresponse to cardiac resynchronization therapy. *Circulation* 2014;**130**:87–90.
171. Parsai C, Bijnens B, Sutherland GR, Baltabaeva A, Claus P, Marciniak M *et al*. Toward understanding response to cardiac resynchronization therapy: left ventricular dyssynchrony is only one of multiple mechanisms. *Eur Heart J* 2009;**30**:940–9.
172. Parsai C, Baltabaeva A, Anderson L, Chaparro M, Bijnens B, Sutherland GR. Low-dose dobutamine stress echo to quantify the degree of remodelling after cardiac resynchronization therapy. *Eur Heart J* 2009;**30**:950–8.
173. Stankovic I, Aarones M, Smith HJ, Vörös G, Kongsgaard E, Neskovic AN *et al*. Dynamic relationship of left-ventricular dyssynchrony and contractile reserve in patients undergoing cardiac resynchronization therapy. *Eur Heart J* 2014;**35**:48–55.
174. Voigt JU, Schneider TM, Korder S, Szulik M, Gürel E, Daniel WG *et al*. Apical transverse motion as surrogate parameter to determine regional left ventricular function inhomogeneities: a new, integrative approach to left ventricular asynchrony assessment. *Eur Heart J* 2009;**30**:959–68.
175. Ghani A, Delnoy PP, Smit JJ, Ottervanger JP, Ramdat Misier AR, Adiyaman A *et al*. Association of apical rocking with super-response to cardiac resynchronization therapy. *Neth Heart J* 2016;**24**:39–46.
176. Stankovic I, Prinz C, Ciarka A, Daraban AM, Mo Y, Aarones M *et al*. Long-term outcome after CRT in the presence of mechanical dyssynchrony seen with chronic RV pacing or intrinsic LBBB. *JACC Cardiovasc Imaging* 2017;**10**(10 Pt A):1091–9.
177. Bazoukis G, Thomopoulos C, Tse G, Tsioufis K, Nihoyannopoulos P. Global longitudinal strain predicts responders after cardiac resynchronization therapy—a systematic review and meta-analysis. *Heart Fail Rev* 2022;**27**:827–36.
178. Menet A, Bernard A, Tribouilloy C, Leclercq C, Gevaert C, Guyomar Y *et al*. Clinical significance of septal deformation patterns in heart failure patients receiving cardiac resynchronization therapy. *Eur Heart J Cardiovasc Imaging* 2017;**18**:1388–97.
179. Salden OAE, Zweerink A, Wouters P, Allaart CP, Geelhoed B, de Lange FJ *et al*. The value of septal rebound stretch analysis for the prediction of volumetric response to cardiac resynchronization therapy. *Eur Heart J Cardiovasc Imaging* 2021;**22**:37–45.
180. De Boeck BW, Teske AJ, Meine M, Leenders GE, Cramer MJ, Prinzen FW *et al*. Septal rebound stretch reflects the functional substrate to cardiac resynchronization therapy and predicts volumetric and neurohormonal response. *Eur J Heart Fail* 2009;**11**:863–71.
181. Russell K, Eriksen M, Aaberge L, Wilhelmssen N, Skulstad H, Remme EW *et al*. A novel clinical method for quantification of regional left ventricular pressure-strain loop area: a non-invasive index of myocardial work. *Eur Heart J* 2012;**33**:724–33.
182. Cvijic M, Duchenne J, Ünü S, Michalski B, Aarones M, Winter S *et al*. Timing of myocardial shortening determines left ventricular regional myocardial work and regional remodelling in hearts with conduction delays. *Eur Heart J Cardiovasc Imaging* 2018;**19**:941–9.
183. Vecera J, Penicka M, Eriksen M, Russell K, Bartunek J, Vanderheyden M *et al*. Wasted septal work in left ventricular dyssynchrony: a novel principle to predict response to cardiac resynchronization therapy. *Eur Heart J Cardiovasc Imaging* 2016;**17**:624–32.
184. Galli E, Leclercq C, Fournet M, Hubert A, Bernard A, Smiseth OA *et al*. Value of myocardial work estimation in the prediction of response to cardiac resynchronization therapy. *J Am Soc Echocardiogr* 2018;**31**:220–30.
185. Duchenne J, Larsen CK, Cvijic M, Galli E, Aalen JM, Klop B *et al*. Visual presence of mechanical dyssynchrony combined with septal scarring identifies responders to cardiac resynchronization therapy. *JACC Cardiovasc Imaging* 2022;**15**:2151–3.
186. Stassen J, Galloo X, Chimed S, Hirasawa K, Marsan NA, Delgado V *et al*. Clinical implications of left atrial reverse remodeling after cardiac resynchronization therapy. *Eur Heart J Cardiovasc Imaging* 2022;**23**:730–40.
187. Bouwmeester S, Mast TP, Keulards DCJ, de Lepper AGW, Herold IHF, Dekker LR *et al*. Left atrial reverse remodeling predicts long-term survival after cardiac resynchronization therapy. *J Echocardiogr* 2022;**20**:115–23.
188. van Everdingen WMM, Walmsley J, Cramer MJ, van Hagen I, De Boeck BWL, Meine M *et al*. Echocardiographic prediction of cardiac resynchronization therapy response requires analysis of both mechanical dyssynchrony and right ventricular function: a combined analysis of patient data and computer simulations. *J Am Soc Echocardiogr* 2017;**30**:1012–1020.e2.
189. Burri H, Domenichini G, Sunthorn H, Fleury E, Stettler C, Foulkes I *et al*. Right ventricular systolic function and cardiac resynchronization therapy. *Europace* 2010;**12**:389–94.
190. Leong DP, Höke U, Delgado V, Auger D, Witkowski T, Thijssen J *et al*. Right ventricular function and survival following cardiac resynchronization therapy. *Heart* 2013;**99**:722–8.
191. Stassen J, van der Bijl P, Galloo X, Hirasawa K, Prihadi EA, Marsan NA *et al*. Prognostic implications of right ventricular free wall strain in recipients of cardiac resynchronization therapy. *Am J Cardiol* 2022;**171**:151–8.
192. Campbell P, Takeuchi M, Bourgoun M, Shah A, Foster E, Brown MW *et al*. Right ventricular function, pulmonary pressure estimation, and clinical outcomes in cardiac resynchronization therapy. *Circ Heart Fail* 2013;**6**:435–42.
193. European Heart Rhythm Association (EHRA); European Society of Cardiology (ESC); Heart Rhythm Society; Heart Failure Society of America (HFA); American Society of Echocardiography (ASE); American Heart Association (AHA); European Association of Echocardiography (EAE) of ESC; Heart Failure Association of ESC (HFA), Daubert JC, Saxon L, Adamson PB, Auricchio A, Berger RD, Beshai JF *et al*. 2012

- EHRA/HRS expert consensus statement on cardiac resynchronization therapy in heart failure: implant and follow-up recommendations and management. *Europace* 2012;**14**:1236–86.
194. Biffi M, Massaro G, Diemberger I, Martignani C, Corzani A, Ziacchi M. Cardiac resynchronization therapy in persistent left superior vena cava: can you do it two-leads-only? *HeartRhythm Case Rep* 2016;**3**:30–2.
195. Sidhu BS, Sieniewicz B, Gould J, Elliott MK, Mehta VS, Betts TR et al. Leadless left ventricular endocardial pacing for CRT upgrades in previously failed and high-risk patients in comparison with coronary sinus CRT upgrades. *Europace* 2021;**23**:1577–85.
196. Khan FZ, Virdee MS, Palmer CR, Pugh PJ, O'Halloran D, Elvik M et al. Targeted left ventricular lead placement to guide cardiac resynchronization therapy: the TARGET study: a randomized, controlled trial. *J Am Coll Cardiol* 2012;**59**:1509–18.
197. Döring M, Braunschweig F, Eitel C, Gaspar T, Wetzel U, Nitsche B et al. Individually tailored left ventricular lead placement: lessons from multimodality integration between three-dimensional echocardiography and coronary sinus angiogram. *Europace* 2013;**15**:718–27.
198. Adelstein E, Alam MB, Schwartzman D, Jain S, Marek J, Gorcsan J et al. Effect of echocardiography-guided left ventricular lead placement for cardiac resynchronization therapy on mortality and risk of defibrillator therapy for ventricular arrhythmias in heart failure patients (from the Speckle Tracking Assisted Resynchronization Therapy for Electrode Region [STARTER] trial). *Am J Cardiol* 2014;**113**:1518–152.
199. Kandala J, Upadhyay GA, Altman RK, Parks KA, Orencole M, Mela T et al. QRS Morphology, left ventricular lead location, and clinical outcome in patients receiving cardiac resynchronization therapy. *Eur Heart J* 2013;**34**:2252–62.